NUC TP 505

2

SPHERICAL ACRYLIC PLASTIC HULLS UNDER EXTERNAL EXPLOSIVE LOADING

by

J. D. Stachiw

Ocean Technology Department

March 1976

NAVAL UNDERSEA CENTER, SAN DIEGO, CA. 92132

AN ACTIVITY OF THE NAVAL MATERIAL COMMAND

R. B. GILCHRIST, CAPT, USN
Commander

HOWARD L. BLOOD, PhD
Technical Director

ADMINISTRATIVE INFORMATION

This report describes research performed between June 1973 and June 1975 as part of the investigation into man-rated transparent submersibles. The program was funded under a Project Order from the Naval Material Command through the Independent Research and Independent Exploratory Development program at the Naval Undersea Center under Subproject Task Area Number ZF-61-412-001.

Released by

H. R. Talkington, Head,
Ocean Technology Department

ACKNOWLEDGEMENTS

The testing of model-size and full-size NEMO-type hulls was conducted at Southwest Research Institute. The experimental study owes its achievement to the administrative and moral support of H. R. Talkington, Head, NUC Ocean Technology Department, and Dr. Wm. B. McLean, retired NUC Technical Director.

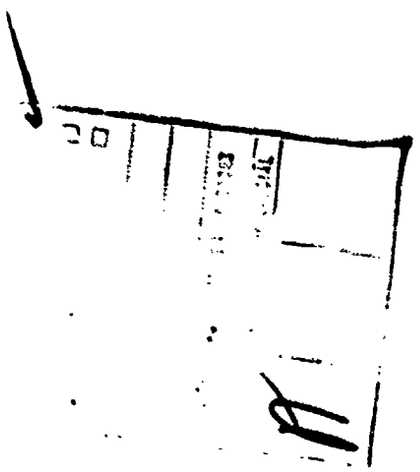

UNCLASSIFIED

SECURITY CLASSIFICATION OF THIS PAGE (When Data Entered)

REPORT DOCUMENTATION PAGE		READ INSTRUCTIONS BEFORE COMPLETING FORM
1. REPORT NUMBER NUC TP 505	2. GOVT ACCESSION NO.	3. RECIPIENT'S CATALOG NUMBER
4. TITLE (and Subtitle) SPHERICAL ACRYLIC PLASTIC HULLS UNDER EXTERNAL EXPLOSIVE LOADING		5. TYPE OF REPORT & PERIOD COVERED Research Report June 1973 -- June 1975 6. PERFORMING ORG. REPORT NUMBER
7. AUTHOR(s) J. D. Stachiw		8. CONTRACT OR GRANT NUMBER(s)
9. PERFORMING ORGANIZATION NAME AND ADDRESS Naval Undersea Center San Diego, California 92132		10. PROGRAM ELEMENT, PROJECT, TASK AREA & WORK UNIT NUMBERS ZF61412001
11. CONTROLLING OFFICE NAME AND ADDRESS Naval Undersea Center San Diego, California 92132		12. REPORT DATE March 1976 13. NUMBER OF PAGES 78
14. MONITORING AGENCY NAME & ADDRESS (if different from Controlling Office)		15. SECURITY CLASS. (of this report) UNCLASSIFIED 15a. DECLASSIFICATION DOWNGRADING SCHEDULE

16. DISTRIBUTION STATEMENT (of this Report)

Approved for public release; distribution unlimited.

17. DISTRIBUTION STATEMENT (of the abstract entered in Block 20, if different from Report)

18. SUPPLEMENTARY NOTES

19. KEY WORDS (Continue on reverse side if necessary and identify by block number)

submersibles
transparent materials
underwater explosions

20. ABSTRACT (Continue on reverse side if necessary and identify by block number)

NEMO-type acrylic spherical hulls have been subjected to underwater explosions in order to determine their resistance to hydrodynamic impulse loading. Six 15-in.-OD and one 66-in.-OD spheres have been subjected to explosions of sufficient magnitude to initiate fracture in the hull. The tests were conducted at simulated depths of 10, 100, 1000, and 2000 ft with explosive charges of 1.1, 8.2, 14.6, 169.9, 387.8, and 688.6 grams.

DD FORM 1 JAN 73 1473 EDITION OF 1 NOV 65 IS OBSOLETE S/N 0102-014-6601

UNCLASSIFIED

SECURITY CLASSIFICATION OF THIS PAGE (When Data Entered)

20. Continued.

The tests have shown that an acrylic sphere will fracture in the 0- to 50-ft depth range under dynamic peak overpressures that are smaller in magnitude than static pressures required for general implosion of the sphere. At the depth that is equal to 0.2 of static implosion pressure, the magnitude of dynamic peak overpressures must be in excess of the static implosion pressure before fracture of the acrylic sphere is initiated.

Fractures were generally initiated on the internal surface of the sphere at two locations: (a) at a point closest to the explosive and (b) at a point farthest from the explosive. The fractures were generally in the shape of a star.

SUMMARY

PROBLEM

Manned submersibles with spherical acrylic plastic hulls have been known since the NEMO hull was designed in 1961 to provide greater panoramic vision at lower cost and weight-to-displacement ratio than steel hulls (of the same shape, size, and depth capability) equipped with many small viewports. Several submersibles with NEMO-type hulls have been built since that time by the U. S. Navy. After more than 5 years of service, the acrylic hulls have been found to be virtually maintenance free and have shown no sign of weathering. There is, however one area of uncertainty that currently restricts the choice of missions for submersibles with acrylic hulls; it is not known how resistant the spherical acrylic hull is to hydrodynamic impulse loadings generated by explosive-actuated tools like cable cutters, stud guns, explosive anchors, corers, and others. If the resistance of NEMO-type hulls to underwater explosions were known acrylic submersibles could be utilized in missions for which explosive tools are mandatory for meeting the mission objective.

RESULTS

An exploratory test program has shown that spherical hulls of acrylic plastic can withstand dynamic impulses of considerable magnitude before fracture of the hull is initiated. Increasing the depth of operations was found to increase significantly the resistance of the acrylic hull to fracture initiation by dynamic impulses. The NEMO Mod 2000 hull, with a 66-in. outside diameter and 4-in. shell thickness, has been found to withstand explosion-generated peak dynamic overpressure of 4,927 psi without initiation of fracture.

RECOMMENDATION

Manned submersibles with NEMO-type spherical hulls of acrylic plastic may be safely utilized in search, rescue, salvage, and work missions where explosive-actuated work tools are routinely utilized for achievement of mission objectives, provided that the peak dynamic overpressure impinging on the acrylic hull is less than 25 percent of static implosion pressure of the hull.

CONTENTS

INTRODUCTION

Underwater visibility is extremely important to crews of submersibles engaged in search, salvage, or work missions. Panoramic visibility can be provided in many ways, but large spherical acrylic plastic windows are considered to provide the most cost effective and reliable way of meeting this operational requirement (Ref. 1). An even better way is to use a transparent acrylic plastic hull of spherical shape (Ref. 2). Not only does it provide unlimited visibility in all directions, but it also generates a significant amount of buoyancy. Furthermore, such a hull is non-magnetic, provides unsurpassed thermal and sound insulation, and is virtually maintenance free. Because of its transparency, it can be inspected for incipient cracks visually by its crew at any time. This feature alone makes acrylic pressure hulls inherently safer than those fabricated from opaque materials that require expensive and time-consuming inspection procedures for detection of cracks.

The performance of spherical acrylic pressure hulls under short-term, long-term, and cyclic pressure loadings has been experimentally established over the years by U. S. Navy (Refs. 3-12) so that submersibles with spherical acrylic plastic hulls can be economically built and operated in the 0- to 3300-ft depth range. Several submersibles with acrylic plastic hulls have been already built and are operating in that depth range (Refs. 13, 14, 15). Their performance record is excellent, and acrylic plastic hulls that have been exposed to sun, seawater, and heat for 6 years still show no signs of deterioration.

In many undersea missions, the submersible may be exposed to explosions generated intentionally by, for example the firing of a stud gun or cable cutter during a typical underwater work sequence. During some missions, the submersible may be subjected to severe explosions unintentionally, e.g., during recovery or neutralization of underwater ordnance (Ref. 1). The effect of underwater explosions on submersible hulls made of steel is fairly well understood and the resistance to dynamic overpressures can be readily calculated. This is not the case with acrylic plastic pressure hulls or large spherical sector windows.

This report summarizes findings from the first exploratory study conducted by the U. S. Navy on the effect of underwater explosions on acrylic plastic spherical hulls of NEMO-type design and construction.

DESCRIPTION OF STUDY

The objective of the study was to provide operators of existing acrylic plastic submersibles (NEMO, Makakai, Johnson-Sea-Link I and Johnson-Sea-Link II) with operational guidelines for missions in which the submersible may be exposed to underwater explosions.

The approach selected for meeting the objective of the study was experimental in nature. It was felt that the experimental approach was, in this case, more direct, more reliable, and less expensive than an analytical approach, which would, subsequently, have to be experimentally validated before it could be used with confidence by operators of submersibles.

The scope of the study was limited to spherical hulls of NEMO design and construction with 1000 and 3000 ft maximum operational depths. Only two sizes of hulls were to be tested: the 66-in.-OD full-size and the 15-in.-OD scale-size spheres. The NEMO-type design uses a sphere with two penetrations located at opposite poles of the sphere; each penetration is closed with a metallic closure equipped with a conical seating surface. In NEMO-type construction, the sphere is assembled from 12 spherical-sector pentagons bonded together with self-polymerizing acrylic cement.

EXPERIMENTAL DESIGN

TEST SPECIMENS

Two NEMO capsules, one 66-in.-OD full-size and six 15-in.-OD scale-size, served as test specimens (Figs. 1 and 2). Both NEMO Mod 600 with 1000-ft operational depth and NEMO Mod 2000 with 3000-ft operational depth were utilized (Table 1 and Appendix A). Both the full-size and scale-size NEMO capsules have been exposed previously to cyclic fatigue testing and thus can be considered to be equivalent to submersibles with several years of field service (Ref. 11).

All specimens were fabricated from Plexiglas G, whose physical properties met the U. S. Navy and ASME requirements. The spherical hulls were assembled in every case from thermoformed spherical pentagons that were bonded together with either PS-18 or PS-30 self-polymerizing adhesive. The scale-size hulls had polar inserts machined either from stainless steel or titanium (Figs. 3-6), while the full-size hull utilized aluminum, both for top hatch and bottom penetration plate (Fig. 7).

TEST ARRANGEMENT

Scale-Size NEMO Capsules

The testing of scale-size models took place in a 30-in.-ID pressure vessel, 20 ft long, located at the Southwest Research Institute. The test specimen was placed in a test jig that held it approximately 120 in. below the end closure and 120 in. above the bottom closure (Fig. 8). To prevent point contact between the test specimen and the steel test jig, the specimen was wrapped in a wire net that, in turn, was fastened to the three longitudinal members of the test jig.

The explosive was suspended above the test specimen by means of two horizontal wires stretched between the longitudinal members of the test jig. It was centered directly above the center of the test specimen, with the standoff being defined as the distance between the center of explosive and the outer surface of the test specimen facing the charge (Fig. 9).

The instrumentation consisted solely of two tourmaline piezoelectric transducers for measurement of dynamic overpressures. The transducers were positioned adjacent to the model and were the same distance from the explosive charge as was the outer surface of the model. Transducer response was transmitted through differential amplifiers and displayed on a dual-beam oscilloscope, where it was photographed. It was considered advantageous to

use two transducer systems so that the validity of pulse characteristics could be ascertained by noting the similarity in response of the two independent monitoring systems.

The output of the piezoelectric transducers was displayed on an oscilloscope and recorded photographically by a Polaroid camera. The oscilloscope was triggered by a small breakwire wrapped around the charge. The breaking of the wire by the explosion generated a pulse which energized the oscilloscope for a single sweep. In initial tests, a time-delay pulse generator was not available, so the sweep speed of the oscilloscope had to be such that transducer response to shock overpressure was appropriately displayed during the single sweep. In later tests, by using a delayed trigger pulse, it was possible to eliminate the initial straight-line portion of the display and obtain greater detail of shock-pulse characteristics.

Full-Size NEMO Capsules

Testing of the full-size NEMO Mod 2000 capsule took place in a 12-ft-diameter, 100-ft-deep, water-filled well located on the premises of Southwest Research Institute (Fig. 10). The test specimen was securely wrapped with Nylon webbing and suspended within a steel cage by means of steel cables (Fig. 11). The cage itself was kept suspended at 50 ft depth by means of a cable attached to a large mobile crane.

For the first three shots, the explosive (Fig. 12) was held above the test specimen. For the subsequent two tests it was placed below the test specimen. Changing the location of the explosive was made necessary by the generation of large downward force upon the crane by pressure waves radiating from explosive held above the specimen. When the explosive was placed below the specimen, the pressure wave would tend to decrease the load on the crane, rather than increase it.

Instrumentation consisted of two electric resistance strain gages and two pressure-sensitive transducers. The strain gages were mounted on the interior of the hull midway between the polar inserts and directly below the explosive.

The pressure transducers, PCB Model 113A23 acceleration-compensated ultra-rigid quartz element pressure probes with built-in amplifiers, were positioned the same distance from the explosive charge as the apex of the test specimen (Fig. 13). Pressure gage outputs were displayed on a Tektronix Model 454 split-beam oscilloscope, and strain gage outputs were displayed on a Tektronix Model 502 dual-beam oscilloscope. Both scopes were set to trigger in a single sweep mode, with the trace being recorded on Polaroid film. A small-diameter breakwire, wrapped around the charge, broke when the charge detonated, thereby creating a voltage change and triggering the oscilloscopes; the scope sweeps were delayed by a time slightly less than the time required for an acoustic pulse in water to travel the distance between the charge and the apex of the model.

TEST PROCEDURE

Scale-Size NEMO Capsules

Each of the scale-size NEMO capsules were tested individually. Since the objective of the testing program for scale-size capsules was to determine the effect of the depth and capsule shell thickness on the resistance of capsules to damage caused by dynamic overpressure, some of the test parameters, like sizes of explosive charges and standoff distances, were

kept constant. The sizes of charges chosen were 1.1, 8.2 and 14.6 grams. Standoff distances were set at 48, 36, 24 and 12 in.

The procedure (Tables 2 and 3) followed during testing of any given test specimen was to start with the smallest charge (1.1 grams) placed at the longest standoff distance (48 in.). If no damage to the test specimen was observed, an identical charge would be placed at the next shorter standoff distance (36 in.). The standoff distances chosen for each shot were progressively shorter until the shortest standoff (12 in.) was reached.

If the smallest charge did not initiate failure of the test specimen at the shortest standoff distance, the next larger charge (8.2 grams) would be placed at the longest standoff. The larger charges would be set off following the test procedure already described for the smallest charge. If the larger charge did not initiate cracks at the shortest standoff, the series of tests would be repeated again, utilizing, however, the largest charge (14.6 grams).

The 15-in.-OD by 14-in.-ID scale-size NEMO test specimens were tested at simulated depths of 10, 100, or 1000 ft. The 10-ft depth represented the typical surface cruising depth of a submersible, while 1000 ft represented maximum operational depth of NEMO capsules with $t/R_o = 0.067$ ratio.

The 15-in.-OD by 13-in.-ID scale-size NEMO test specimens were tested at depths of 10, 100, or 2000 ft. Here again, 10 ft represented the typical surface cruising depth, while 1000 and 2000 ft represented depths of typical deep submergence operational missions.

Full-Size NEMO Capsules

The test procedure for full-size capsules (Table 4) differed from the test procedure used for scale-size capsules. While for scale-size capsules both the size of the charge and the standoff distance were experimental variables, for the full-size capsule only the charge size was varied, while the standoff was held constant at 52.8 in. This standoff distance was determined by multiplying the shortest standoff distance of 12 in. by 66.15, the ratio representing the relationship between the size of the full-size NEMO and that of the scale-size NEMO.

The charge weights used against the full-size NEMO capsule were 1.1, 5.6, 14.5, 169.9, 387.8, and 688.6 grams. The first three charges were of the same weight as those used in the explosive testing of scale-size NEMO capsules. They were used primarily to calibrate pressure transducers and strain gage readout equipment. The last three charges were scaled-up versions of charges previously used against scale-model NEMOs. Thus, the 169.9-gram charge is the scaled-up version of the 1.1-gram charge, the 387.8-gram charge is the scaled-up version of 4.6-gram charge, and the 688.6-gram charge is the scaled-up version of 8.25-gram charge. The scaled-up charges were supposed to generate the same peak overpressures on the full-scale NEMO from a $0.8R_o$ standoff as were generated previously on the scale-size NEMO capsules from a $0.8r_o$ standoff by 1.1-, 4.6-, and 8.2-gram charges.*

*R_o external radius of the full size NEMO

*r_o external radius of the scale size NEMO

TEST OBSERVATIONS

Scale-Size NEMO Capsules

The testing of the scale-size NEMO capsules was very destructive to the 30-in. pressure vessel in which the testing was conducted. Seals in the vessel end closures as well as hydraulic piping were repeatedly damaged. Because of it, seals and hydraulic fittings had to be replaced every second or third shot.

Pressure transducers were also damaged repeatedly. After several days of testing, the project ran out of transducers, and further shots were conducted without any instrumentation. Thus, for some of the shots during which the capsules failed, both the peak overpressure and the impulse intensity had to be calculated. There is, however, a very high confidence in the calculated values, since it was found that during the shots in which instrumentation functioned, the correlation between calculated and experimental values was quite good (Figs. 14, 15, 16, and 17).

Failure of model-size NEMO capsules was manifested by formation of either tensile- or flexure-type cracks. As a rule, the flexure cracks were present on the interior surface of the equator directly facing the charge, on the opposite side, or on both sides, while the tensile cracks extended radially from the edges of penetrations. If the underwater explosion was severe, there would be several long flexure-type cracks joined together in a form of a star, very similar in appearance to the pattern of cracks observed in spherical sector windows under point impact loading (Ref. 16). Severe explosions would also generate tensile meridional cracks at the penetrations.

Light damage was observed on test specimens J and 26 (Figs. 18 and 19). In both cases, there were only one or two small flexure cracks at the equator, no leakage of water took place and the capsule was considered to have withstood the explosion without endangering its potential cargo. These capsules could have completed their mission successfully.

Medium severe damage was noted on test specimens M and 24 (Figs. 20 and 21). In both cases, there were several short flexure cracks present at the equator and at least one long tensile crack at the penetration. Only a few drops of water leaked into the interiors of the capsules, but not in sufficient quantity to endanger the potential cargo. Still, the missions of the capsules would have to be terminated immediately to avoid endangering the crew.

Very severe damage was observed on test specimens K and 25 (Figs. 22 and 23). In both cases, a large star-shaped flexure crack at the equator and several tensile cracks radiating from penetrations were produced. Because of the many cracks, water leaked into the interiors of these two capsules. There would have been severe jeopardy for any cargo. It is very probable that capsules in such condition could not return from their missions since they would fill with water prior to reaching the mother ship.

Full-Size NEMO Capsule

The full-size NEMO capsule withstood all the explosions without initiation of cracks in the acrylic plastic. However, during the last three shots, the capsule was torn loose from its fastenings. On the last shot, the capsule broke free of its 0.25-in. steel cable netting and

rose rapidly to the surface of the well shaft, where it struck a protruding steel beam. The point impact broke off a large chip from the capsule surface, thus terminating any further tests on this capsule (Fig. 24).

Dynamic strains measured on the interior of the capsule facing the 387.8-gram charge indicated considerable tension immediately followed by compression of approximately the same magnitude (Fig. 25). Still, the strains were not of such magnitude as to suggest failure during the following 688.6-gm shot.

Dynamic pressure readings were obtained only with the initial two small charges (Figs. 26 and 27). No experimental pressure readings were obtained with the following four larger charges because the breaking loose of the capsule destroyed, in every case, the pressure pickups and associated wiring. However, such a good correlation was obtained between the experimental and calculated peak overpressure values during the initial shots that peak overpressures for the last three shots could be calculated with confidence.

DISCUSSION OF TEST RESULTS

Although the data generated during the testing program are far from complete, several definite relationships between the force of explosion and capsule's resistance to failure can be formulated.

EFFECT OF SHELL THICKNESS

It appears that the resistance to fracture of acrylic plastic spheres subjected to underwater explosions is directly related to shell thickness, provided that the method of construction and outside radius remain the same. This postulate is based on the observation that to initiate cracking in 1-in.-thick scale-size NEMO capsules required a unit impulse and peak dynamic overpressure twice as large as those required to produce similar results in 0.5-in.-thick capsules. Both tests were conducted at the same depth. For example, test specimen No. 26 with a 0.5-in.-thick wall failed at 1000 ft under 0.1 psi.-sec unit impulse and 2816 psi peak dynamic overpressure, while test specimen No. K with 1.0 in.-thick wall required 0.206 psi-sec unit impulse and 6176 psi peak dynamic overpressure to initiate cracking at the same depth. A similar relationship can be seen, although less clearly, between specimen No. 25 and No. M.

EFFECT OF DEPTH

The data show quite clearly that the resistance to fracture of acrylic plastic spheres subjected to underwater explosions increases significantly with depth. This conclusion is based on the observation that it required a 3 to 5 times larger peak overpressure and unit impulse to fracture an identical test specimen at 1000 ft depth than it did at 10 ft. For example, test specimen No. M failed at 10 ft depth under 0.045 psi-sec unit impulse, and 1434 psi peak dynamic overpressure, while test specimen No. K at 1000 ft depth required 0.206 psi-sec unit impulse and 6176 psi peak dynamic overpressure to generate a fracture. Similar relationship can be seen between specimen No. 25 and No. 26.

EFFECT OF SCALING

There are insufficient experimental data to establish the validity of using scale-size models for determining the resistance of full-size NEMO capsules to underwater explosions. The few data points generated during the study seem to indicate, however, that extrapolating data from scale-size models is on the conservative side and, thus, acceptable. This conclusion is based on the observation that the full-size NEMO capsule did not crack when subjected to peak dynamic overpressure of 4927 psi generated by a 688.56-gm charge with $0.8R_o$ standoff, while the same peak dynamic overpressure generated by a scaled-down charge of 8.2 gm with $0.8\ r_o$ standoff would, without a doubt, have cracked the 15-in.-OD by 13-in.-ID scale-size NEMO capsule.

EFFECT OF MOUNTING

During the testing of model-size capsules, there was no problem with retaining the capsules inside the test jig to which they were mounted. The mounting, which consisted of chicken wire mesh wrapped around the capsule and fastened securely with wires to the jig frame, was substantial and capable of withstanding the thrust exerted upon the capsule by dynamic pressure. This was not the case with the full-size NEMO capsule. Although the nylon netting was substantial, and the net was fastened to the frame with 0.25-in. steel cables, the thrust exerted by dynamic pressure upon the 66-in.-diameter capsule was much higher than what the cables could withstand As a result, the capsule was torn loose from its mounting during the firing of shots No. 4, 5, and 6. (Table 4)

The beneficial effect of depth on the resistance of pressure hulls to dynamic overpressure has been previously observed in other brittle materials besides acrylic plastic, materials whose tensile strength is significantly less than their compressive strength, e.g., glass, ceramics, and concrete. The beneficial effect of depth derives its action from the compressive membrane prestressing imposed on the hull by the static external pressure loading. The compressive prestress must be overcome by the tensile flexure stress generated by the underwater explosion before the brittle material can fail in tension on the interior surface of the hull.

Needless to say, imposing compressive prestress on the hull by static external pressure has its limits for all brittle materials. The limit for the beneficial depth effect is reached when the material in the pressure hull begins to fail during dynamic pressure loading in compression rather than in tension. This happens when the *sum of the dynamic compressive stress* (equal in magnitude to, and following immediately after, the tensile flexure stress phase) *and static compressive stress* exceeds either the yield or ultimate compressive strength (depending on which one is the smaller value) of the brittle material.

For acrylic plastic hulls designed to fail by general plastic instability, the maximum allowable depth for static precompression purposes is approximately 25 to 30 percent of their short-term critical pressure (based on compressive strains generated in the hull after 8 hours of sustained loading at maximum operational depth). Since the maximum operational depth of acrylic hulls is, as a rule, set at 25 to 30 percent of their short-term critical pressure, the beneficial depth effect is active through the whole depth range of operations for acrylic submersibles.

The breaking loose of the full-size NEMO from its mounting as a result of underwater explosion points up to a very serious practical problem for a submersible containing a NEMO capsule. It appears that unless the NEMO capsule is restrained in some very ingenious manner, the primary damage to the acrylic capsule will be caused either by impact against the framework of the submersible after the capsule has broken loose from a weak mounting, or by excessive dynamic stresses generated by very strong, but rigid mounting. Since the NEMO capsules are generally attached to the submersible framework by their metallic end closures, it is highly probable that when subjected to a severe underwater explosion, the capsule will crack around the penetrations because of unacceptably high bearing stresses. For this reason, it is desirable that the capsule also be supported at other locations by large elastomeric pads that would tend to distribute and absorb some of the capsule's thrust caused by impulse loading.

FINDINGS

1. Acrylic plastic spherical pressure hulls will fracture when exposed to underwater explosions whose peak dynamic overpressure may be less than the static critical pressure of the hull.

2. Underwater explosions generate cracks primarily on the interior surface of the sphere at locations directly facing and opposite the charge.

3. Cracks on the interior surface of the sphere indicate localized external dynamic pressure loading, very similar to a mechanical point-impact loading (Ref. 16).

4. Dynamic strains measured on the interior shell surface facing the charge alternate rapidly from tension to compression.

5. Increasing the thickness of the acrylic plastic sphere also increases its resistance to underwater explosions; doubling the thickness appears to double the unit impulse and peak dynamic overpressure required for crack initiation.

6. Increasing the depth of operation also increases the resistance of the acrylic plastic sphere to underwater explosions; increasing the depth by 1000 feet appears to at least triple the unit impulse and peak dynamic overpressure required for crack initiation.

7. Mountings for acrylic plastic spheres tend to fail sooner than the spheres themselves when subjected to underwater explosions.

CONCLUSIONS

Submersibles with NEMO-type acrylic plastic spherical hulls can successfully withstand underwater explosions of considerable magnitude. Increasing the depth of operation significantly increases the resistance of spherical acrylic plastic hull to underwater explosions.

RECOMMENDATIONS

Operational

Submersibles with spherical acrylic plastic pressure hulls should not be exposed to underwater explosions of such magnitude that cracks will be initiated in the hull, or the whole hull torn away from its mounting in the submersible structure. This means that (a) the explosive charges in cable cutters or stud drivers carried routinely by an acrylic plastic submersible should not exceed a certain size if the tools are to be activated in the immediate vicinity of the submersible, and (b) the submersible should not be involved in search missions for unexploded underwater ordnance whose warhead exceeds a critical size for given underwater visibility (i.e., good visibility allows discovery of an unexploded item of ordnance without getting close to it, while poor visibility requires the submersible to be almost in physical contact with the item of ordnance before it is recognized as such).

The maximum sizes of permissible explosive charges for work tools or devices carried routinely by a work submersible have been calculated (Ref. 19) on the basis of the largest charge used in the testing program against full-size NEMO Mod 2000 at 50 ft depth that did no damage to the hull or its mounting (Shot No. 3 of Table 4). Charges *equal to, or less than* those shown in Fig. 28 can be used repeatedly in performance of work missions in the 10- to 3000-ft depth range by a submersible equipped with NEMO Mod 2000 (Ref. 11) or 2000B hull (Ref. 12) ($t/R_o \geq 0.121$).

The minimum safe standoff distance for missions involving search and/or disposal of underwater ordnance have been calculated (Ref. 19) on the basis of the largest charge used in the testing program against full-size NEMO Mod 2000 at 50 ft depth that did no damage to the hull but considerable damage to the capsule mounting (Shot No. 6 of Table 4). Standoff distances *equal to or larger* than those shown in Fig. 29 must be maintained between the submersible with NEMO Mod 2000 or 2000B hull and the unexploded underwater ordnance in the 50- to 3000-ft depth range if fracture of the acrylic hull due to explosion is to be avoided. The standoff distances shown in Fig. 29 are very conservative for depths in excess of 1000 ft.

It is understood, however, that unless a mounting is provided that is capable of restraining the NEMO Mod 2000 hull against a thrust of at least 10^6 lb, the hull may be torn loose from its mounting when subjected to the explosions and standoff distances shown in Fig. 29.

Design

Typical mountings for work submersibles with NEMO Mod 2000 or 2000B acrylic hulls are generally configured (Fig. 30) to withstand forces generated only by vertical buoyancy or dead weight and horizontal hydrodynamic drag of the sphere. The magnitudes of these forces are low, approximately 3000 lb vertical static force and 1000 lb horizontal drag. Since, however, the submersible is also subjected to dynamic forces during docking and retrieval, a well-designed mounting will, as a minimum, restrain an acrylic hull against 100,000 lb of downward thrust, 100,000 lb horizontal thrust, and 16,000 lb vertical pull (for some types of mountings the vertical pull is also about 100,000 lb).

Unfortunately, even well-designed mountings for typical work missions do not provide adequate restraint against severe underwater explosions at the standoffs plotted in Fig. 29. To withstand the thrust of severe explosions, the mountings must be designed with this specific objective in mind. Unfortunately, proven mounting designs do not exist at the present time for submersibles with acrylic spheres routinely engaged in missions in which severe underwater explosions may be encountered. A conceptual design for such service has been prepared, however, and is shown in Fig. 31.

Although Figs. 28 and 29 have been developed specifically for NEMO Mod 2000 and 2000B acrylic plastic hulls, they are also applicable to other acrylic spheres with $t/R_o \geq 0.12$. There is sufficient structural similarity between spheres and spherical sectors with included angle $\alpha \geq 120^\circ$ to make Figs. 28 and 29 applicable also to spherical acrylic plastic sector bow windows in submersibles. Some experimental data exist which confirm this belief.

REFERENCES

1. Naval Civil Engineering Laboratory, Technical Report R-631, Windows for External or Internal Hydrostatic Pressure Vessels; Part 3. Critical Pressure of Acrylic Spherical Shell Windows Under Short-Term Pressure Application, by J. D. Stachiw, F. W. Brier, June 1969 (AD 689789).

2. American Society of Mechanical Engineers, Paper No. 65-WA/UNT-10, "The Design, Fabrication and Testing of Acrylic Pressure Hulls For Manned Vehicles", by J. G. Moldenhauer, J. D. Stachiw, K. Tsuji, November, 1965.

3. Naval Civil Engineering Laboratory, Technical Report R-676, Development of a Spherical Acrylic Plastic Pressure Hull for Hydrospace Application, by J. D. Stachiw, April 1970 (AD 707363).

4. Naval Civil Engineering Laboratory, Technical Note N-1113, The Spherical Acrylic Pressure Hull for Hydrospace Application; Part 2. Experimental Stress Evaluation of Prototype NEMO Capsule, by J. D. Stachiw, K. L. Mack, October 1970 (AD 715772).

5. Naval Civil Engineering Laboratory, Technical Note N-1094, The Spherical Acrylic Pressure Hull for Hydrospace Application; Part 3. Comparison of Experimental and Analytical Stress Evaluations for Prototype NEMO Capsule, by H. Ottsen, March 1970 (AD 709914).

6. Naval Civil Engineering Laboratory, Technical Note N-1134, The Spherical Acrylic Pressure Hull for Hydrospace Application; Part 4. Cyclic Fatigue of NEMO Capsule #3, by J. D. Stachiw, October 1970 (AD 715345).

7. American Society of Mechanical Engineers, Paper No. 70-WA/UnT-6, "The JOHNSON SEA-LINK The First Deep Diving Welded Aluminum Submersible," by R. A. Kelsey and R. B. Dolan, December 1970.

8. Naval Undersea Center, NUC TP 315, Acrylic Plastic Hemispherical shells for NUC Undersea Elevator, by J. D. Stachiw, September 1972 (AD 749029).

9. Naval Undersea Center, NUC TP 383, Cast Acrylic Dome for Undersea Applications, by J. D. Stachiw, January 1974.

10. Naval Undersea Center, NUC TP 410, Development of a Precision Casting Process for Acrylic Plastic Spherical Shell Windows Applicable to High-Pressure Service, by J. D. Stachiw, May 1974.

11. Naval Undersea Center, NUC TP 451, NEMO Mod 2000 Acrylic Plastic Spherical Hull for Manned Submersible Operation At Depths to 3000 ft, by J. D. Stachiw, December 1974.

12. Naval Undersea Center, NUC TP 493, Development of Economical Casting Process for NEMO Type Acrylic Pressure Hulls, by J. D. Stachiw, December 1975.

13. Naval Civil Engineering Laboratory, Technical Report R-749, NEMO, A New Concept in Submersibles, P. K. Rockwell, R. E. Elliott, M. R. Snoey, November 1971 (AD 735103).

14 American Society of Mechanical Engineers, Paper No. 72-WA/OCT-8, "Transparent Hull Submersible MAKAKAI," by D. W. Murphy and W. F. Mazzone, December 1972.

15. American Society of Mechanical Engineers, Paper No. 71-WA/UnT-6, "Acrylic Pressure Hull for JOHNSON SEA-LINK Submersible," by J. R. Maison and J. D. Stachiw, December 1971.

16. Naval Undersea Center, NUC TP 486, Acrylic Plastic Spherical Shell Windows Under Point Impact Loading, by J. D. Stachiw and O. Burnside, July 1975.

17. Naval Undersea Center, NUC TP 393, Glass or Ceramic Spherical Shell Window Assembly for 20,000 psi Operational Pressure, by J. D. Stachiw, May 1974.

18. Naval Undersea Center, NUC TP 355, Flanged Acrylic Plastic Hemispherical Shells for Undersea Systems, by J. D. Stachiw, August 1973 (AD 769213).

19. R. H. Cole, *Underwater Explosions*, Dover Publications, Inc., New York, 1965.

TABLE 1. ACRYLIC PLASTIC SPHERES SERVING AS TEST SPECIMENS

	Outside Diameter, in.	Inside Diameter, in.	Top		Bottom		Short-term static critical pressure,* psi
			Penetration minor diameter (included angle)	Inserts	Penetration minor diameter (included angle)	Inserts	
Model 24	15	14	4.793 in. 40°	316 stainless steel hatch no gasket	4.793 in. 40°	316 stainless steel hatch no gasket	1,650
Model 25	15	14	5.150 in. 43°	316 stainless steel hatch polycarbonate gasket	5.150 in. 43°	acrylic plastic spherical sector no gasket	1,650
Model 26	15	14	5.150 in. 43°	acrylic plastic spherical sector no gasket	no penetration	no hatch no gasket	1,650
Model J	15	13	5.285 in. 48°	6A14V titanium hatch polycarbonate gasket	4.445 in. 40°	6A14V titanium hatch no gasket	4,750
Model K	15	13	5.285 in. 48°	6A14V titanium hatch polycarbonate gasket	4.445 in. 40°	6A14V titanium hatch no gasket	4,750

*Based on experimental data from previous studies (Refs. 3, 11).

TABLE 1. ACRYLIC PLASTIC SPHERES SERVING AS TEST SPECIMENS (Continued)

	Outside Diameter, in.	Inside Diameter, in.	Top		Bottom		Short-term static critical pressure,* psi
			Penetration minor diameter (included angle)	Inserts	Penetration minor diameter (included angle)	Inserts	
Model M	15	13	5.285 in. 48°	6A14V titanium hatch polycarbonate gasket	4.445 in. 40°	6A14V titanium hatch no gasket	4,750
Model NEMO MOD 2000	66	57.9	23.822 in. 48° 30′	6061-T6 aluminum hatch polycarbonate gasket	21.727 in. 44°	6061-T6 aluminum penetration plate polycarbonate gasket	4,750

*Based on experimental data from previous studies (Refs. 3, 11).

TABLE 2. RESISTANCE OF 15-in.-O.D. BY 14-in.-I.D. NEMO SCALE MODELS TO DYNAMIC PRESSURE IMPULSES

Size of Charge, grams	Model 25 10 ft Depth	Model 24 100 ft Depth	Model 26 1000 ft Depth
	Standoff, in.		
1.1	48	48	48
	36	36	36
	24	24	24
	12	12	12
8.2	48.†	48	48
	1035. psi peak overpressure	36	36
	0.033 psi-sec unit impulse	24 **	24
	Severe cracking of hull at equator facing and opposite charge; also severe radial cracks around the penetrations (Fig. 23)	2250. psi peak overpressure 0.067 psi-sec unit impulse Minor meridional cracks near penetrations facing and opposite charge. (Fig. 21)	
14.6			48
			36
			24 *
			2816 psi peak overpressure 0.1 psi-sec unit impulse
			Small crack on equator opposite charge. (Fig. 19)

Notes:
- *The standoff is measured between the tip of the charge and the surface of the NEMO model*
- *Explosive used is cast explosive composed of 50% PETN and 50% TNT*
- *Failure is indicated by presence of cracks.*
- *Shock wave parameters are calculated values*

*Denotes light damage
**Denotes medium severe damage
†Denotes very severe damage

TABLE 3. RESISTANCE OF 15-in.-O.D. BY 13-in.-I.D. NEMO SCALE MODELS TO DYNAMIC PRESSURE IMPULSES

Size of Charge, grams	Model M 10 ft Depth	Model K 1000 ft Depth	Model J 2000 ft Depth
	Standoff, in.		
1.1	48	48	48
	36	36	36
	24	24	24
	12	12	12
8.2	48	48	48
	36 **	36	36
	1434 psi peak overpressure	24	24
	0.045 psi-sec unit impulse		
	Cracks on equator facing charge; also radial crack at the penetration. (Fig. 20)		
14.6		48	48
		36	36
		24	24
		12 *	12 *
		6170 psi peak overpressure	6170 psi peak overpressure
		0.208 psi-sec unit impulse	0.208 psi-sec unit
		Star shaped cracks on equator facing charge, also radial crack at penetration. (Fig. 22)	Small incipient cracks on equator facing and opposite the charge. (Fig. 18)

Notes
- *The standoff is measured between the top of the charge and the surface of the NEMO model*
- *Explosive used is cast explosive composed of 50% PETN and 50% TNT*
- *Failure is indicated by presence of cracks*
- *Shockwave parameters are calculated values*

**denotes light damage **denotes medium severe damage *denotes very severe damage*

TABLE 4. RESISTANCE OF 66-in.-O.D. BY 57.90-in.-I.D. FULL-SIZE NEMO MOD 2000 TO DYNAMIC PRESSURE IMPULSES

Shot No.	Size of Charge, grams	Standoff, in.	Peak Overpressure, psi	Unit Impulse psi-sec	Comments
1	1.10*	52.9	435	0.0074	No damage
2	5.62*	52.9	805	0.0228	No damage
3	14.50*	52.9	1,150	0.0436	No damage
4	169.87*	52.9	2,906	0.2347	No damage; capsule broke loose from test jig.
5	387.77**	52.9	3,967	0.412	No damage, capsule broke loose from test jig.
6	688.56**	52.9	4,927	0.611	No damage, capsule broke loose from test jig.

Notes:
- *The standoff is measured between the tip of the charge and the surface of the NEMO capsule.*
- *Explosive used is cast explosive composed of 50% PETN and 50% TNT*
- *Damage is indicated by presence of cracks*
- *Shock wave parameters are calculated values.*
- *All tests were conducted at 50 ft depth.*

**Explosive located above the capsule.*
***Explosive located below the capsule.*

Figure 1. Scale size NEMO type balls tested to destruction under dynamic impulse loading.

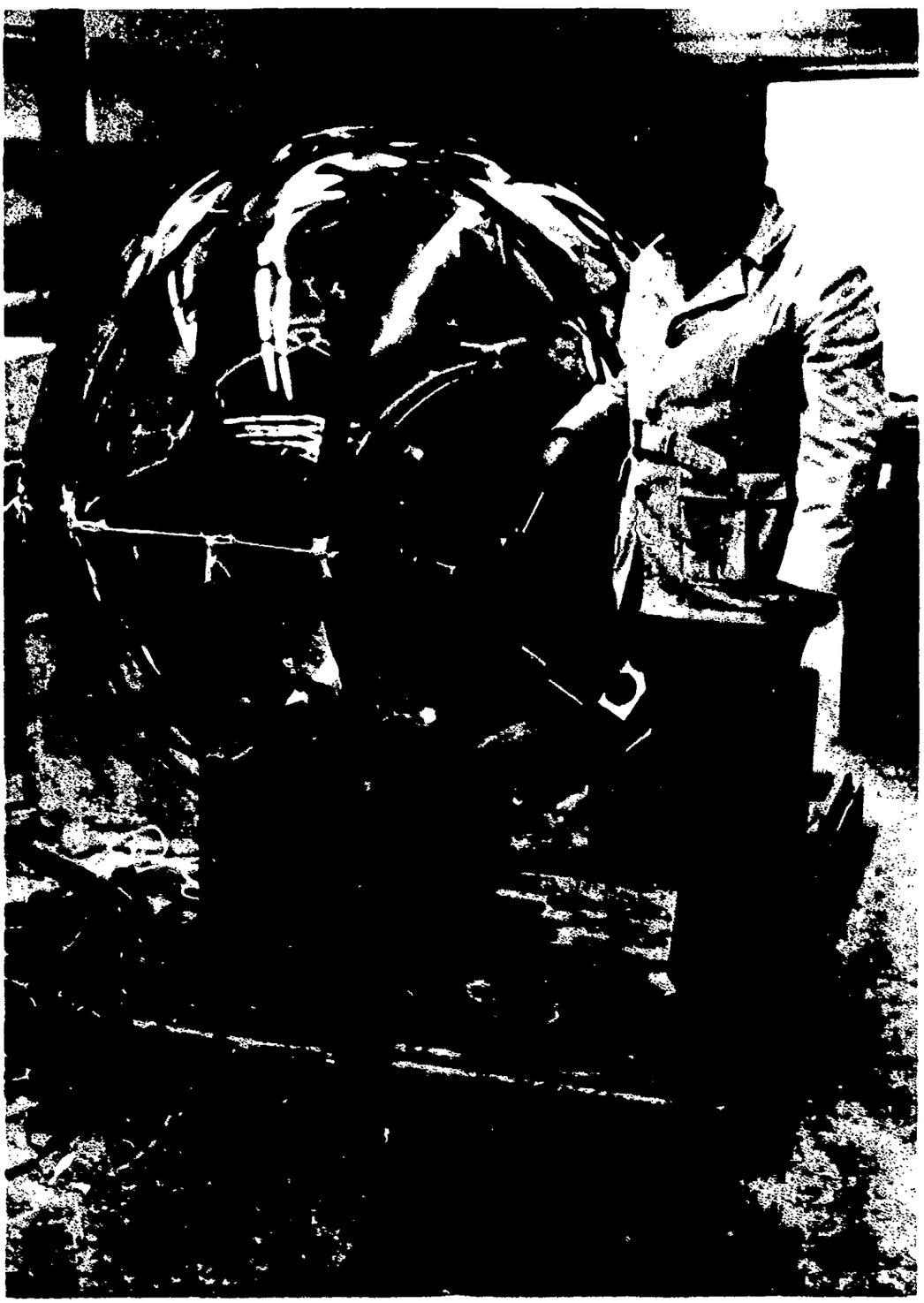

Figure 2. Full-size NEMO Mod 2 [illegible]

APPLICATION				REVISIONS		
NEXT ASSY	USED ON	ZONE	LTR	DESCRIPTION	DATE	APPROVED

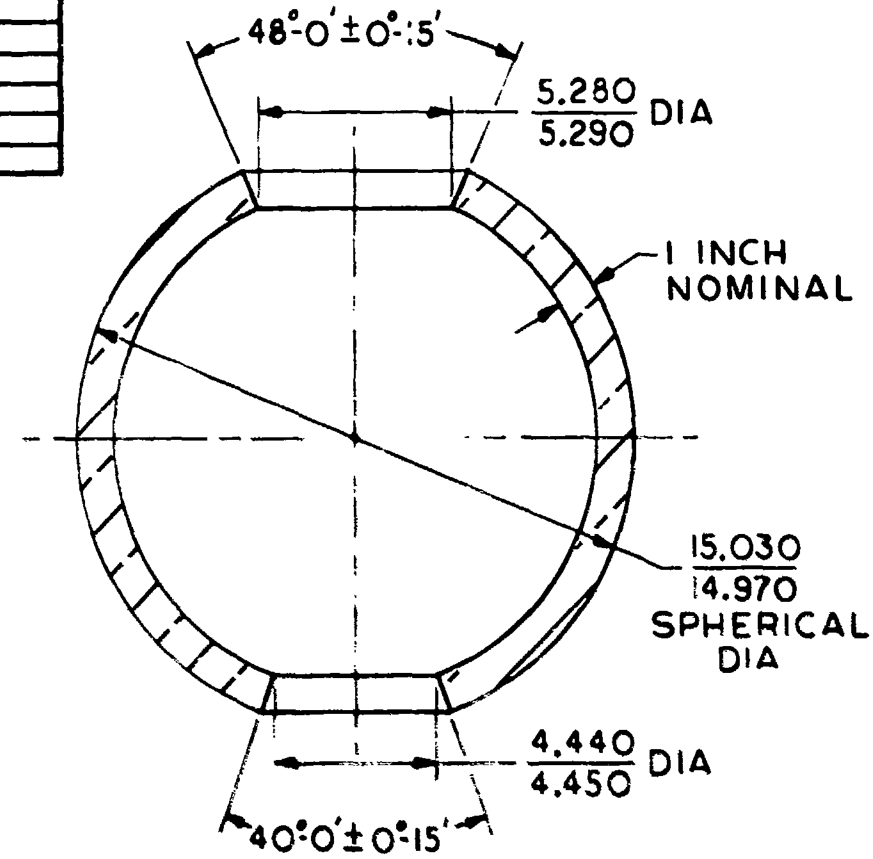

℄ SECTION

NOTES:
1. MATERIAL: PLEXIGLAS G, 1.0 INCH PLATE
2. ADHESIVE: PS-30
3. INSERTS: TOP OPENING - TYPE B TITANIUM HATCH WITH POLYCARBONATE GASKET
BOTTOM OPENING - TYPE A TITANIUM HATCH WITHOUT GASKET

UNLESS OTHERWISE SPECIFIED	NAVAL UNDERSEA CENTER SAN DIEGO, CALIF. 92132 — 10 25 74	DEPARTMENT OF THE NAVY WASHINGTON, D.C. 20360
		NEMO MOD 2000 ACRYLIC HULL 15 INCH NEMO SCALE MODELS #35 #36, & #37
DO NOT SCALE THIS DRAWING		A — 30879 — SK6514-A-0139
		SCALE NONE — SHEET 1 OF 1

11ND-NUC-3910 2A-(2) (11-72)

Figure 3. Typical dimensions of 15 in OD by 13 in ID scale size NEMO [illegible] hulls

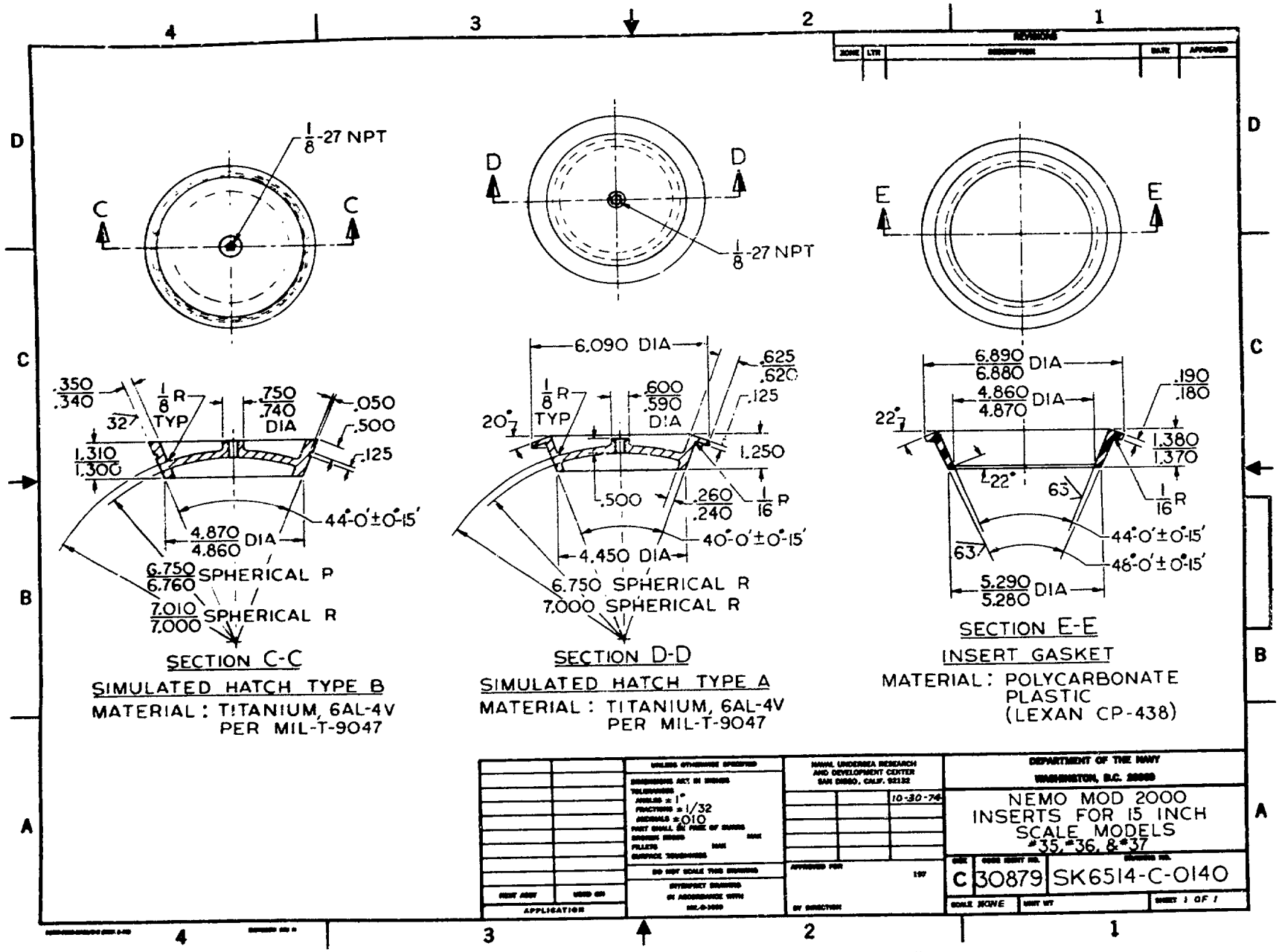

Figure 4. Inserts for penetrations in 15-in.-OD by 13-in.-ID scale-size NEMO-type hulls.

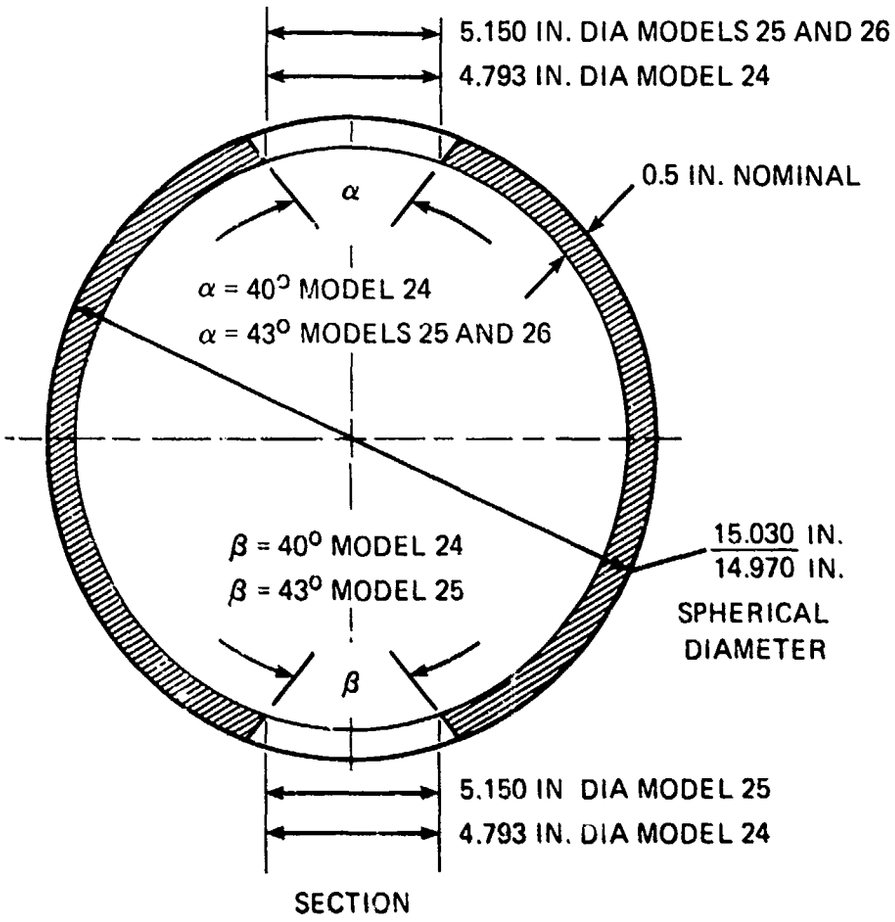

NOTES:

1. MATERIAL: PLEXIGLAS G, 0.5 IN. PLATE
2. ADHESIVE: PS-18

Figure 5. Typical dimensions of 15-in.-OD by 14-in.-ID scale-size NEMO-type hulls.

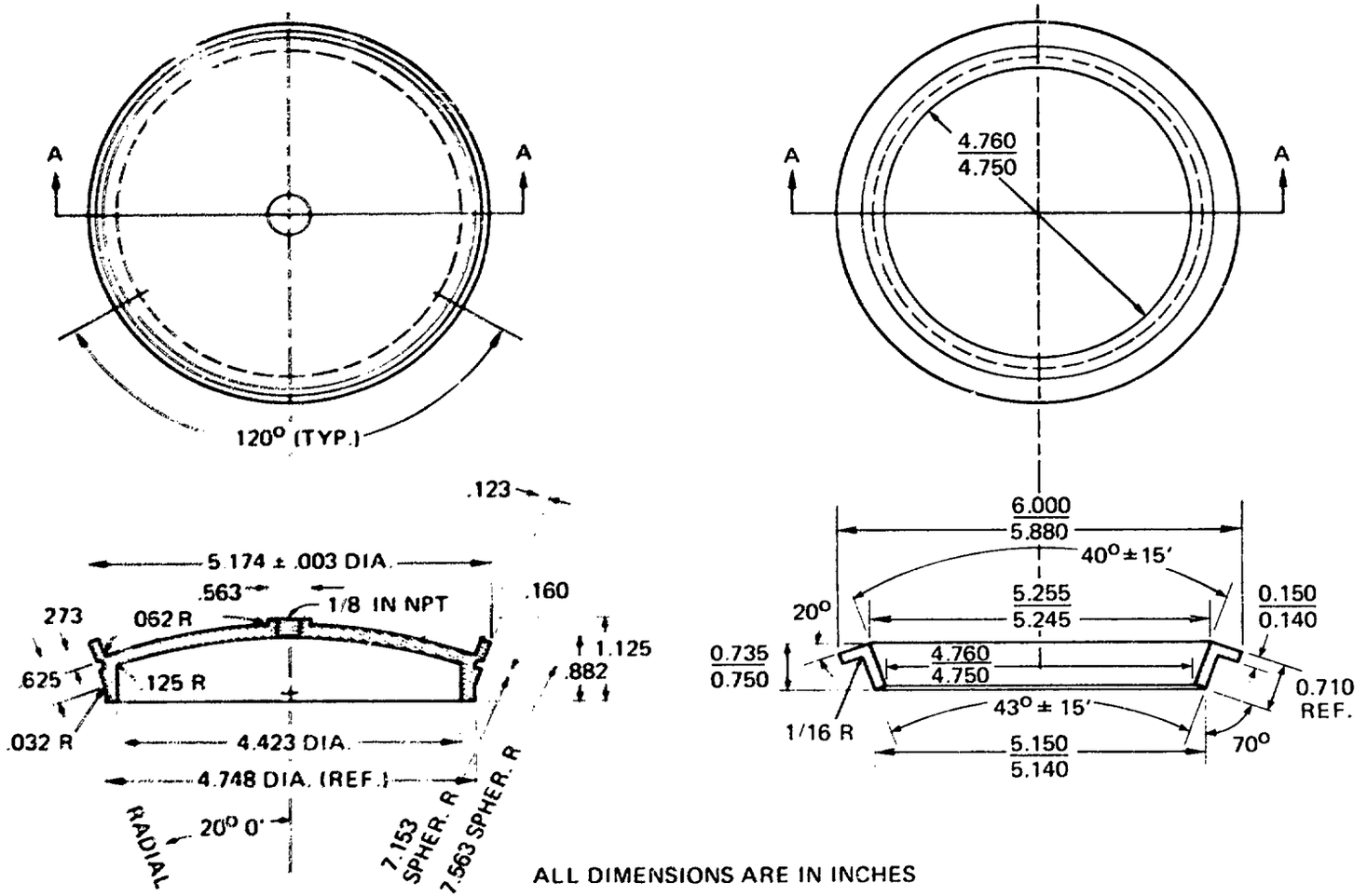

ALL DIMENSIONS ARE IN INCHES

SECTION A–A

SIMULATED HATCH – TYPE C

MATERIAL: 316 STAINLESS STEEL

SECTION A–A

INSERT GASKET

MATERIAL: POLYCARBONATE PLASTIC

Figure 6 Inserts for penetrations in 15-in.-OD by 14-in.-ID scale-size NEMO-type hulls.

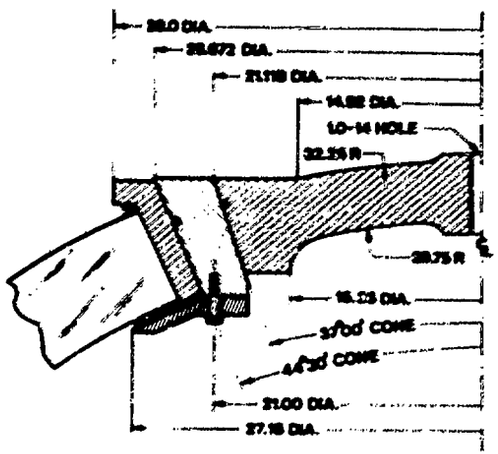

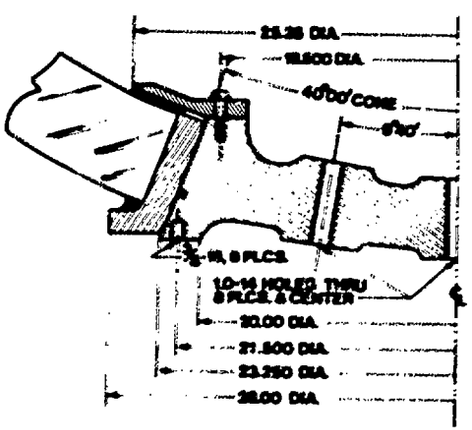

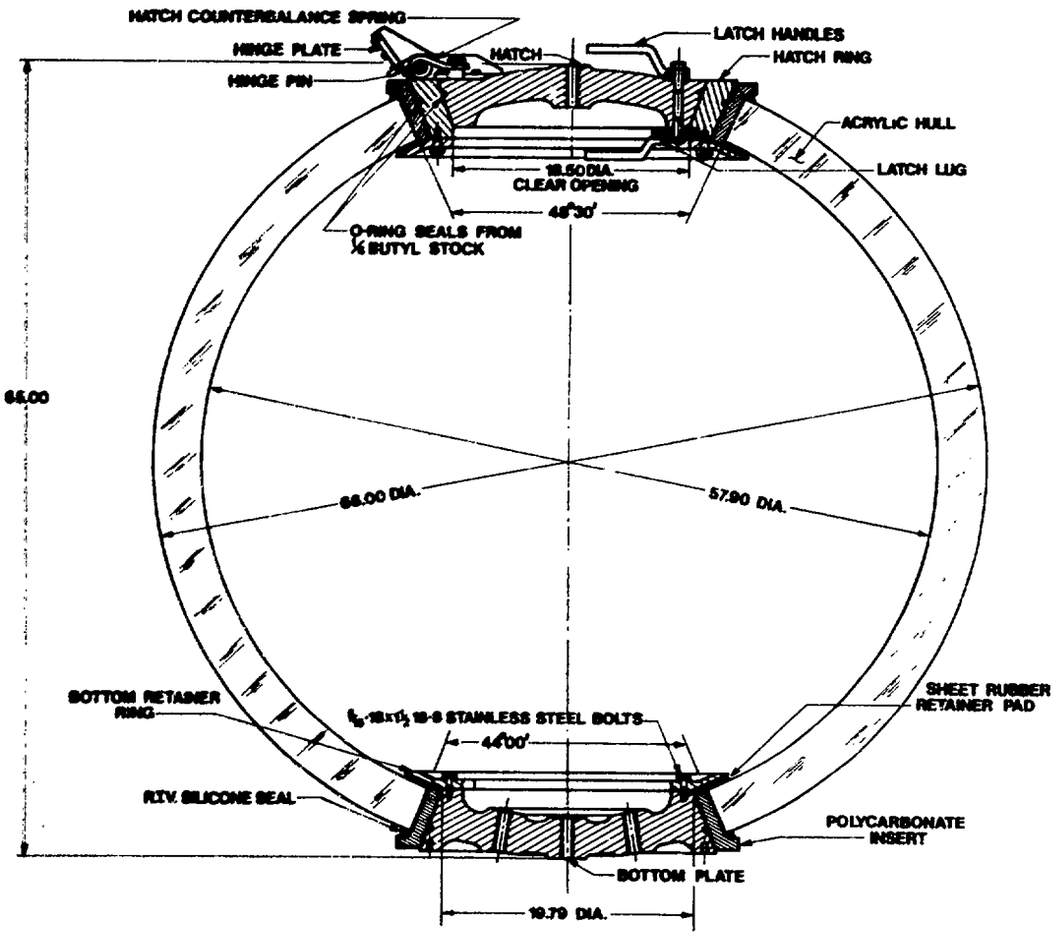

NAVAL UNDERSEA CENTER **ACRYLIC PLASTIC SUBMERSIBLE HULL** **NEMO MODEL 2000** material: plexiglas G acrylic construction: bonded spherical pentagons	weight: 2500 lbs displacement: 5600 lbs cyclic fatigue life: in excess of 1000 dives of 4 hr duration to 3000 ft	operational depth: 3000 ft proof test depth: 3600 ft implosion depth: 10,500 ft positive buoyancy: 3100 lbs weight/displacement: 0.44

Figure 7. Dimensions of 66-in.-OD by 57.9-in.-ID full-size NEMO Mod 2000 capsule.

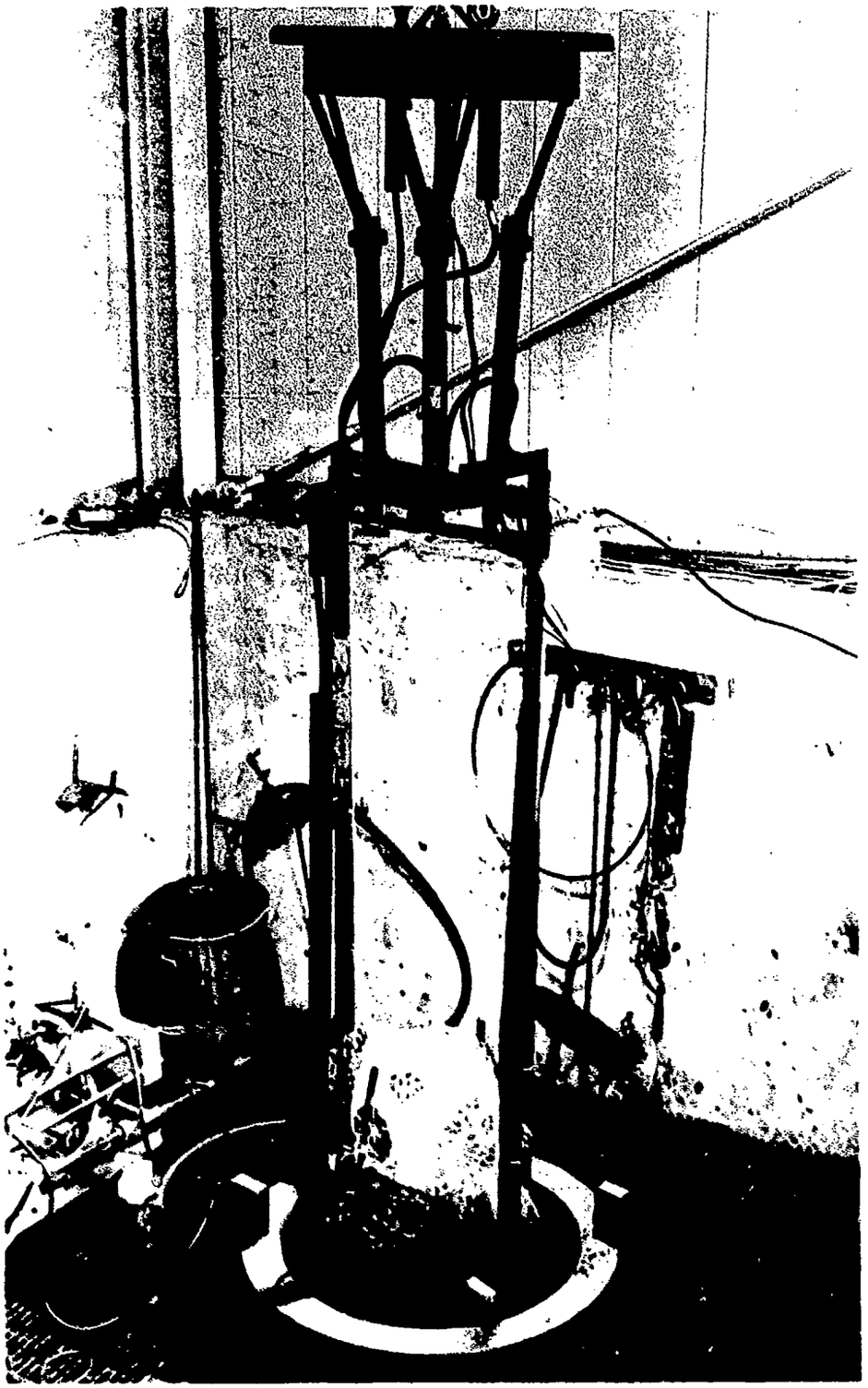

Figure 8. Test rig for holding the scale-size activated capsules in the pressure vessel during detonation of explosive

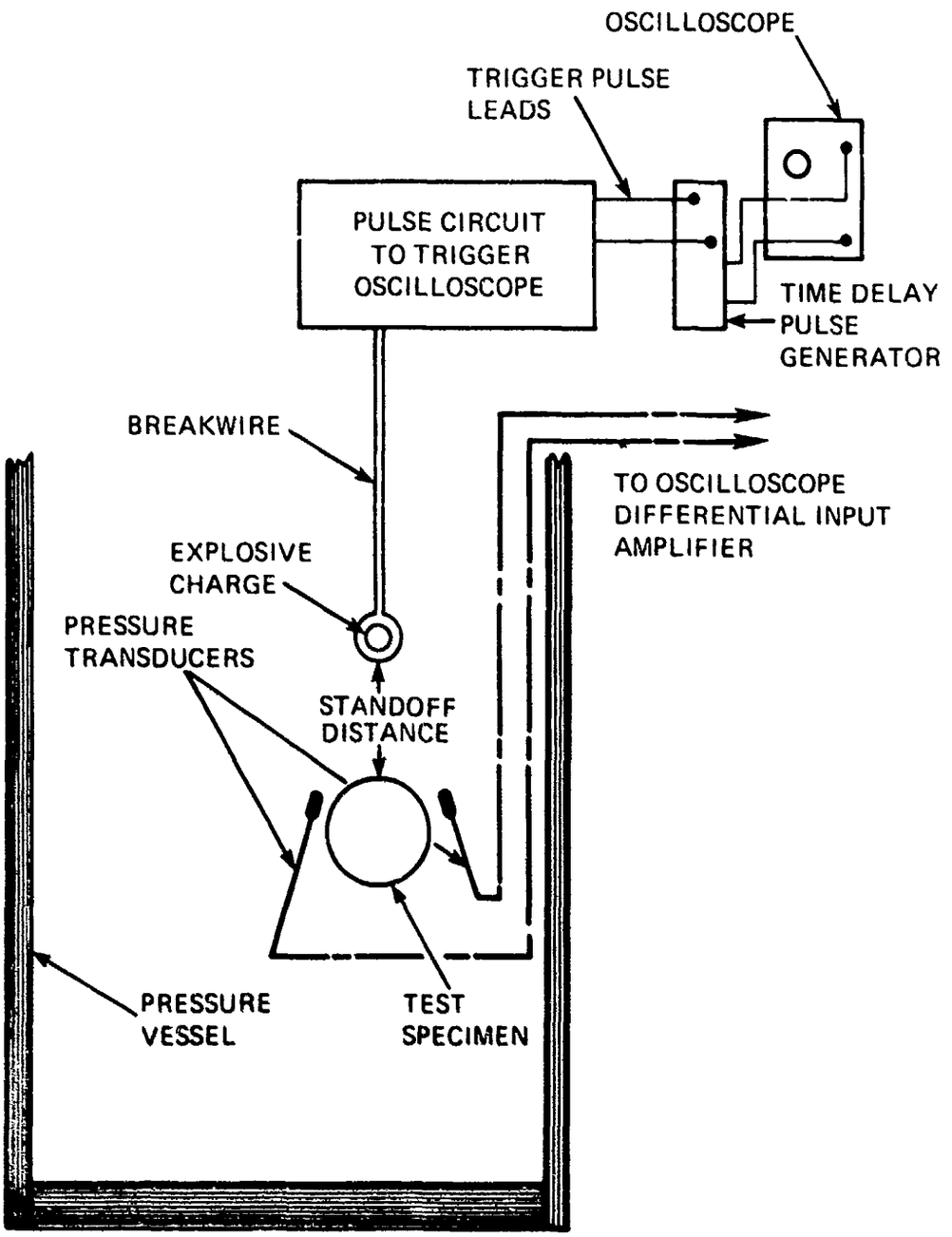

Figure 9. Schematic of instrumentation used for measurement of peak pressure impinging on the acrylic capsules

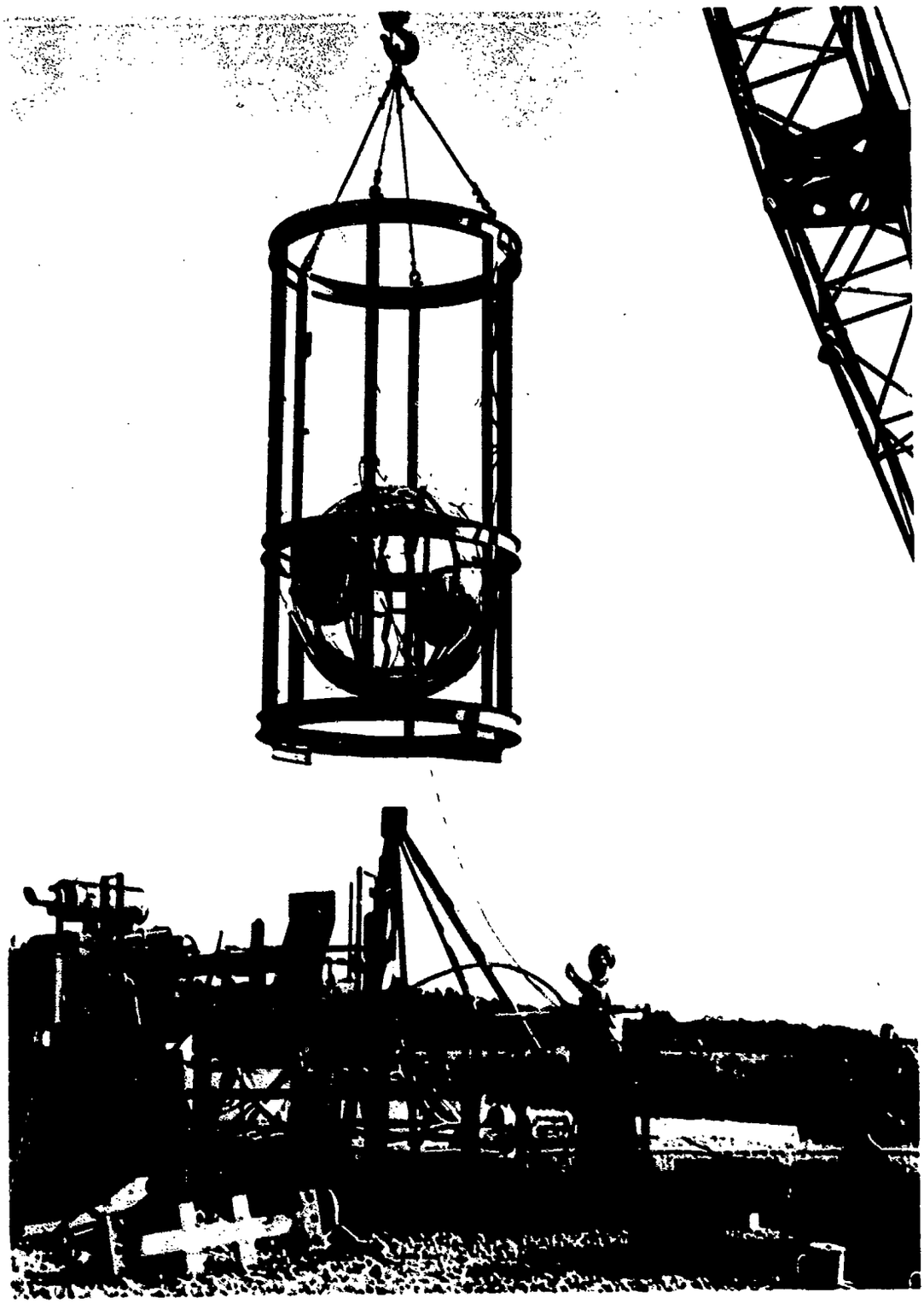

Figure 10. Test rig for holding the full-size NAMO Mod 2000 capsule in the well during detonation of explosive

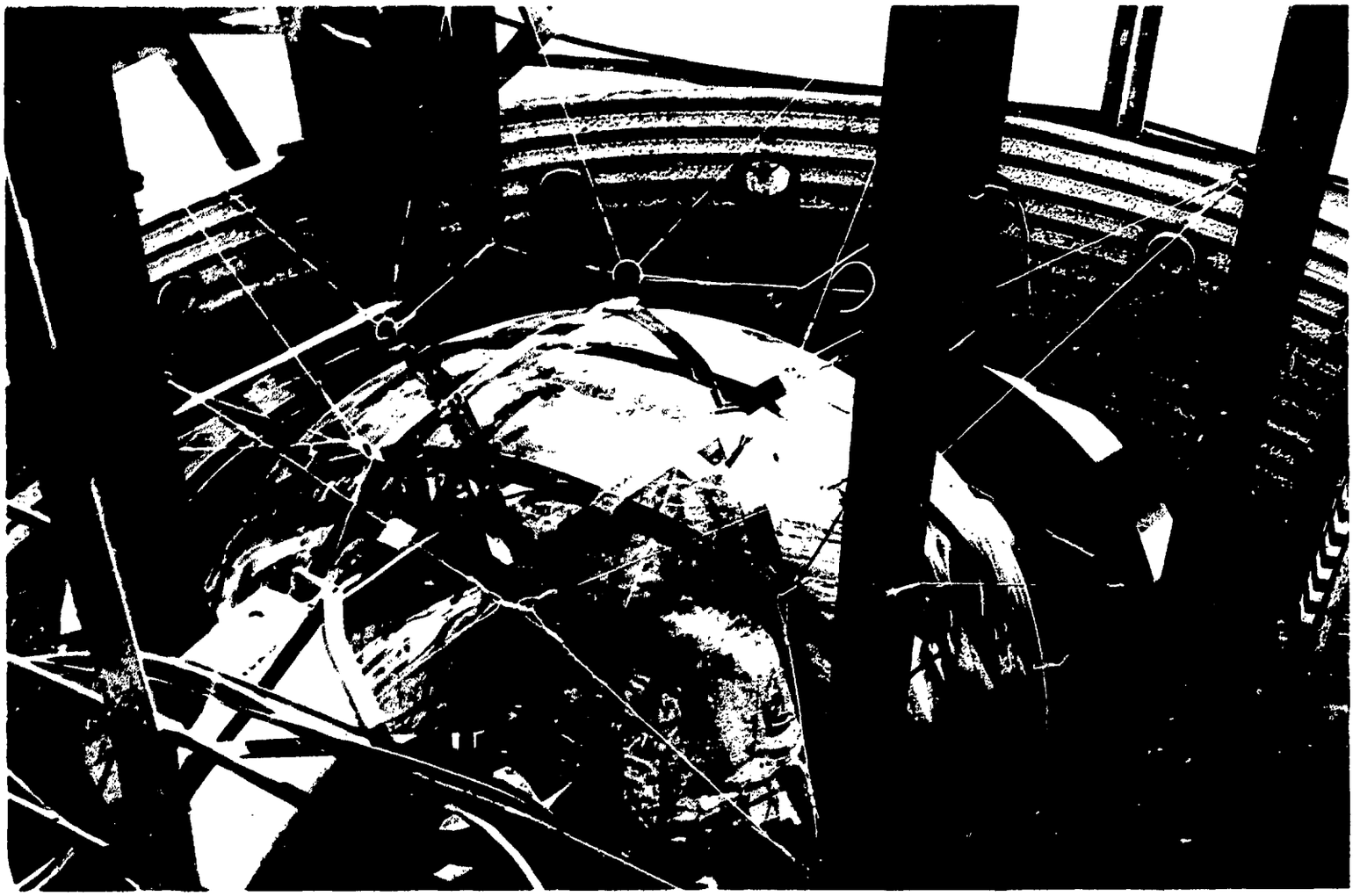

Figure 11 Mounting of the NEMO Mod 2000 capsule inside the test jig.

Figure 12 Typical size and shape of explosive charge used against full-size NIMO Mod 2000 capsule

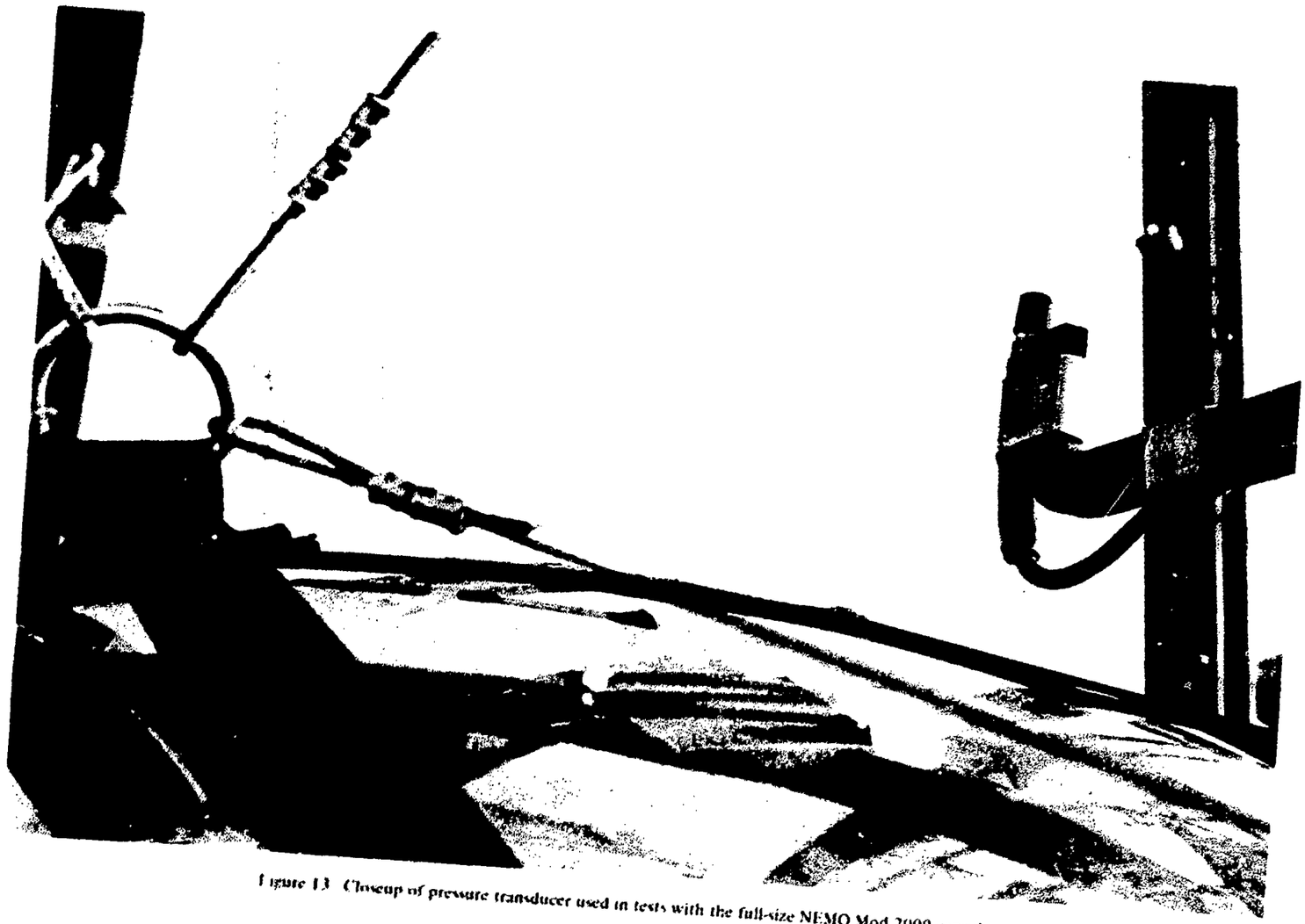

Figure 13. Closeup of pressure transducer used in tests with the full-size NEMO Mod 2000 capsule.

Model: 25 NEMO (15" X 14")

Charge: 8.2 grams

Standoff: 48 inches

Hydrostatic Pressure: 10 psi

	Gage 1	Gage 2	Calculated
Peak Shock Overpressure, psi	1,020	1,035	1,035
Unit Impulse, psi-sec	0.175	0.18	.0325
Duration, μsec	1,350	1,350	--

Note – Model failed.

Figure 14. Peak pressure measured at the scale-size capsule No. 25 during the explosion that fractured the capsule

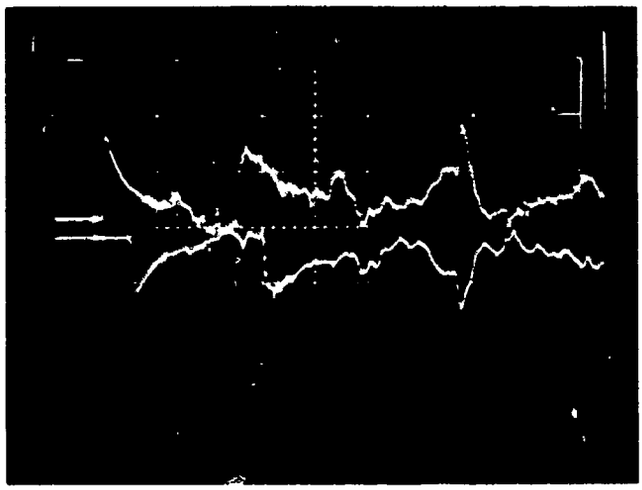

Model: NEMO 26 (15" X 14")

Charge: 14.6 grams

Standoff: 24" (gage 1), 26" (gage 2), 24" (model)

Hydrostatic Pressure: 450 psi

			Calculated	
	Gage 1	Gage 2	Gage 1	Gage 2
Peak Shock Overpressure, psi	2,820	2,250	2,810	2,580
Unit Impulse, psi-sec	.111	.0654	101	.094
Duration, μsec	80	75		

Note Model failed. Gage 2 was farther from model and charge than gage 1 and gives a lower than anticipated value

Figure 15 Peak pressure measured by pressure capsule No. 26 during the explosion that fractured the capsule

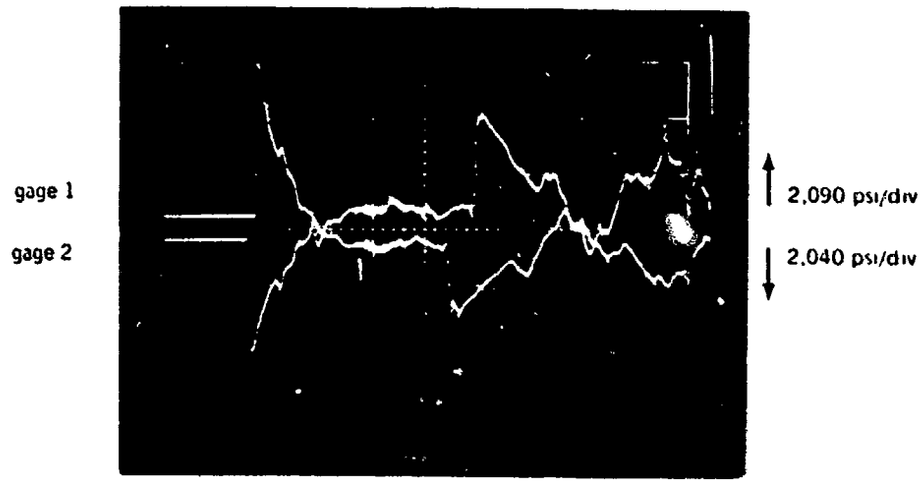

Model: NEMO J (15" X 13")

Charge: 14.6 grams

Standoff: 13" (gage 1), 12" (gage 2), 12" (model)

Hydrostatic Pressure: 1,000 psi

			Calculated	
	Gage 1	Gage 2	Gage 1	Gage 2
Peak Shock Overpressure, psi	5,660	4,430	5,660	6,700
Unit Impulse, psi-sec	1276	1108	194	215
Duration, μsec	50	47.5		

Note Model failed Gage 2 given lower than anticipated value

Figure 16. Peak pressure measured at the scale-size capsule No. 1 during the explosion that fractured the capsule

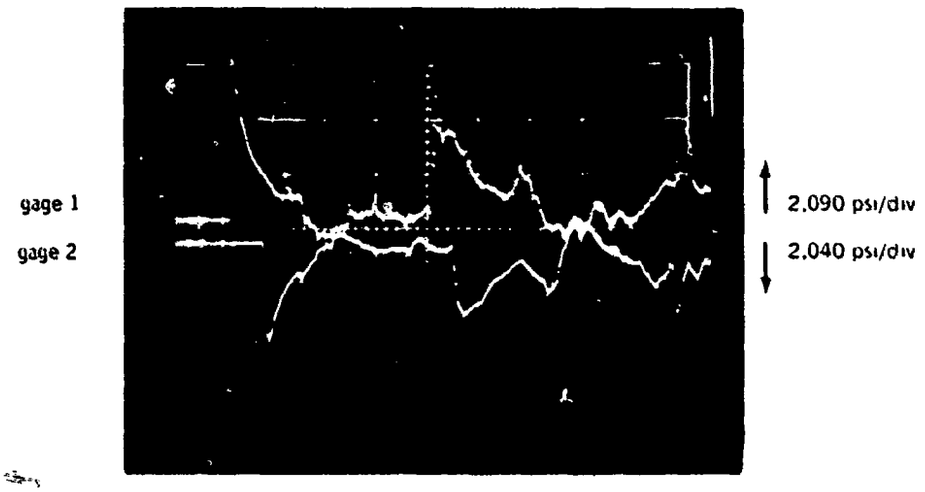

Model: NEMO K (15" X 13")

Charge: 14.6 grams

Standoff: 12" (gage 1), 13" (gage 2), 12" (model)

Hydrostatic Pressure: 450 psi

	Gage 1	Gage 2	Calculated Gage 1	Calculated Gage 2
Peak Shock Overpressure, psi	6,280	4,080	6,200	5,660
Unit Impulse, psi-sec	1856	085	715	194
Duration, μsec	75	50		

Note Model failed Gage 2 reads lower than anticipated.

Figure 17 Peak pressure measured at the underwater capsule No. 4 during the explosion that fractured the capsule

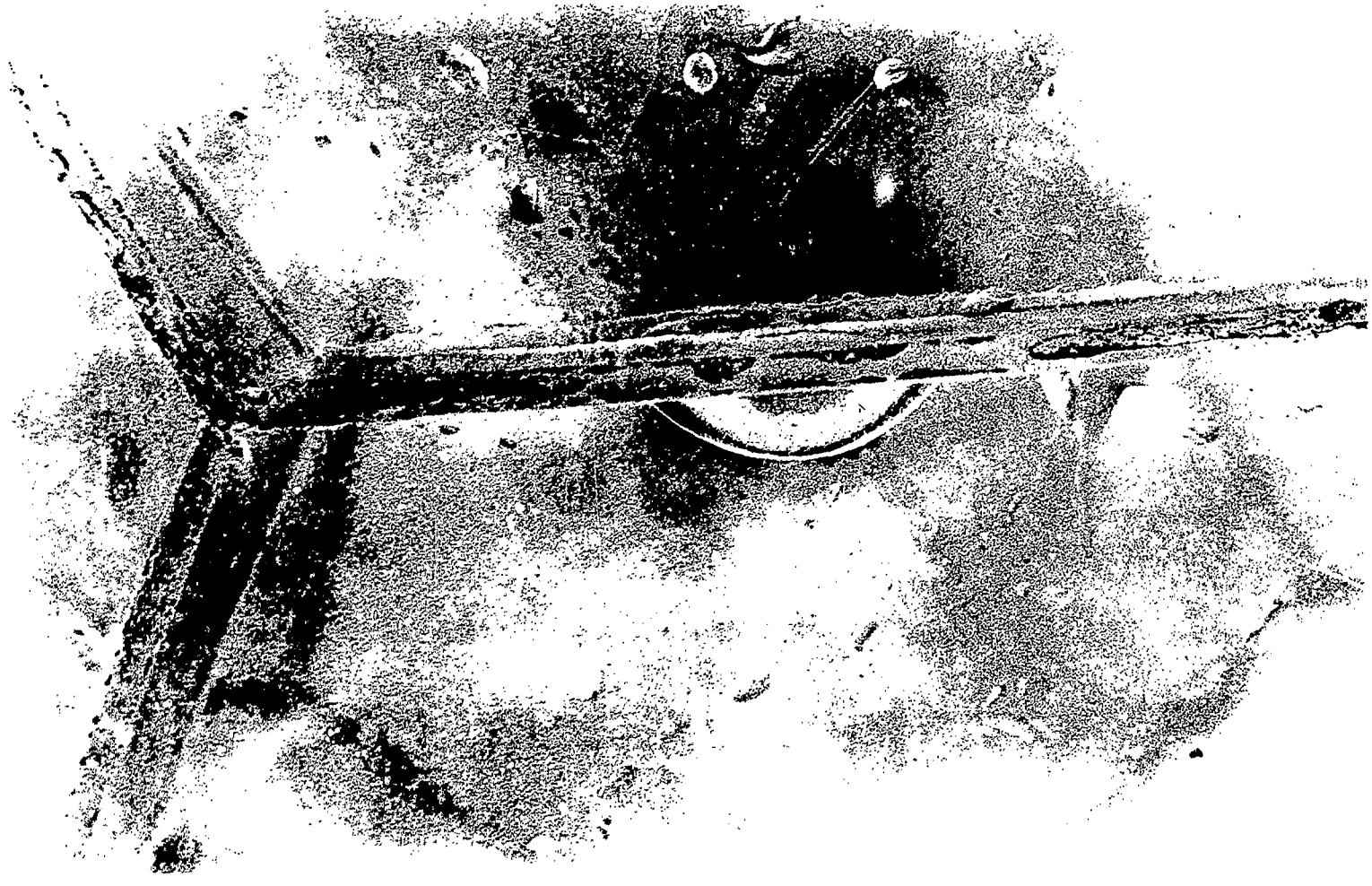

Figure 18. Fractures in capsule No. 1 after being subjected (at 2000-ft depth) to a 14.6-gram charge at 12 in. standoff: (a) crack is facing the explosive. (Sheet 1 of 2)

Figure 18. Fractures in capsule No. 1 after being subjected (at 2000-ft depth) to a 14.6-gram charge at 12 in. standoff; obstruck is on the opposite side of capsule. (Sheet 2 of 21

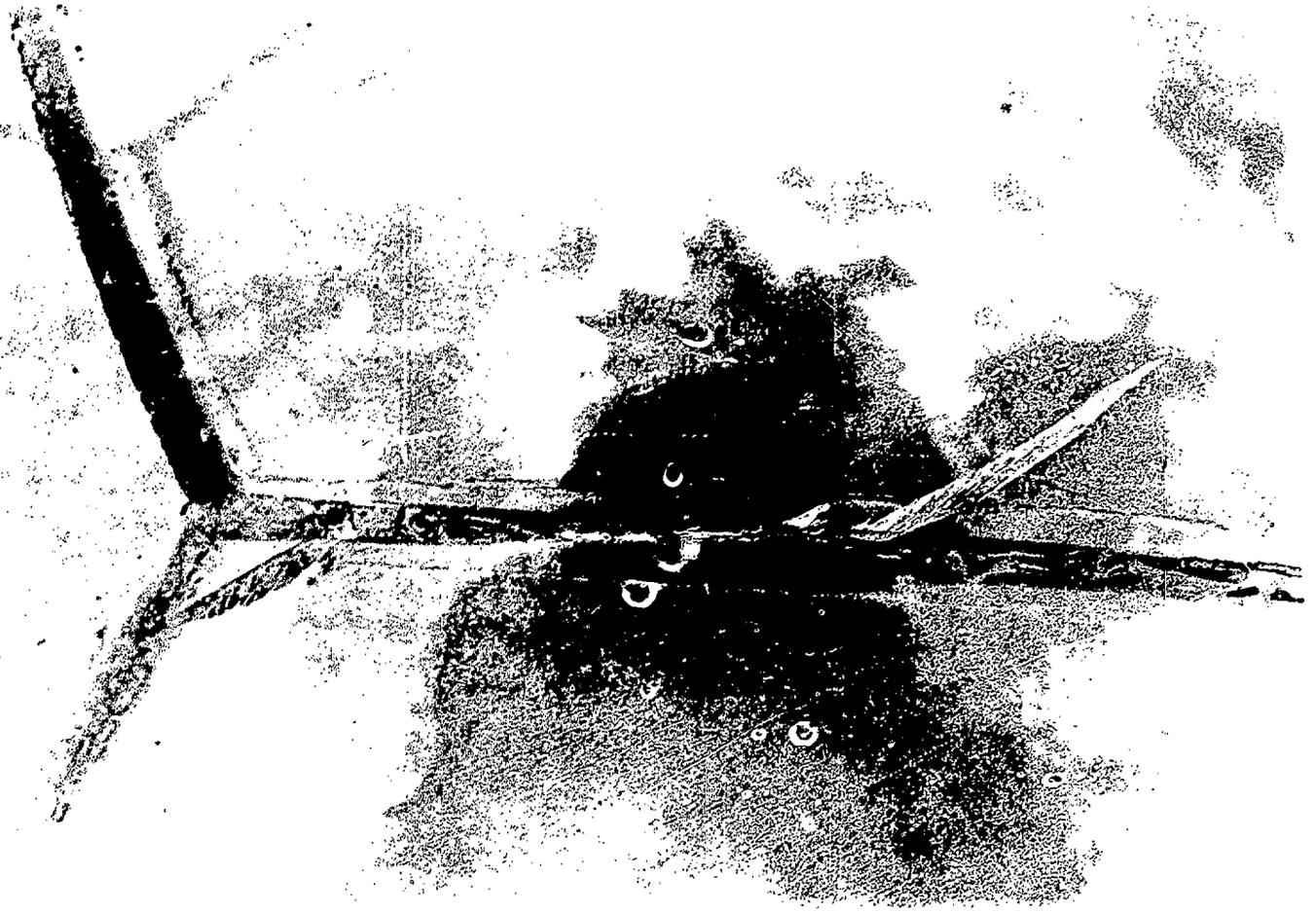

Figure 19. Fracture in capsule No. 26 after being subjected (at 1000-ft depth) to a 14.6-gram charge at 24 in. standoff. Crack is facing the explosive.

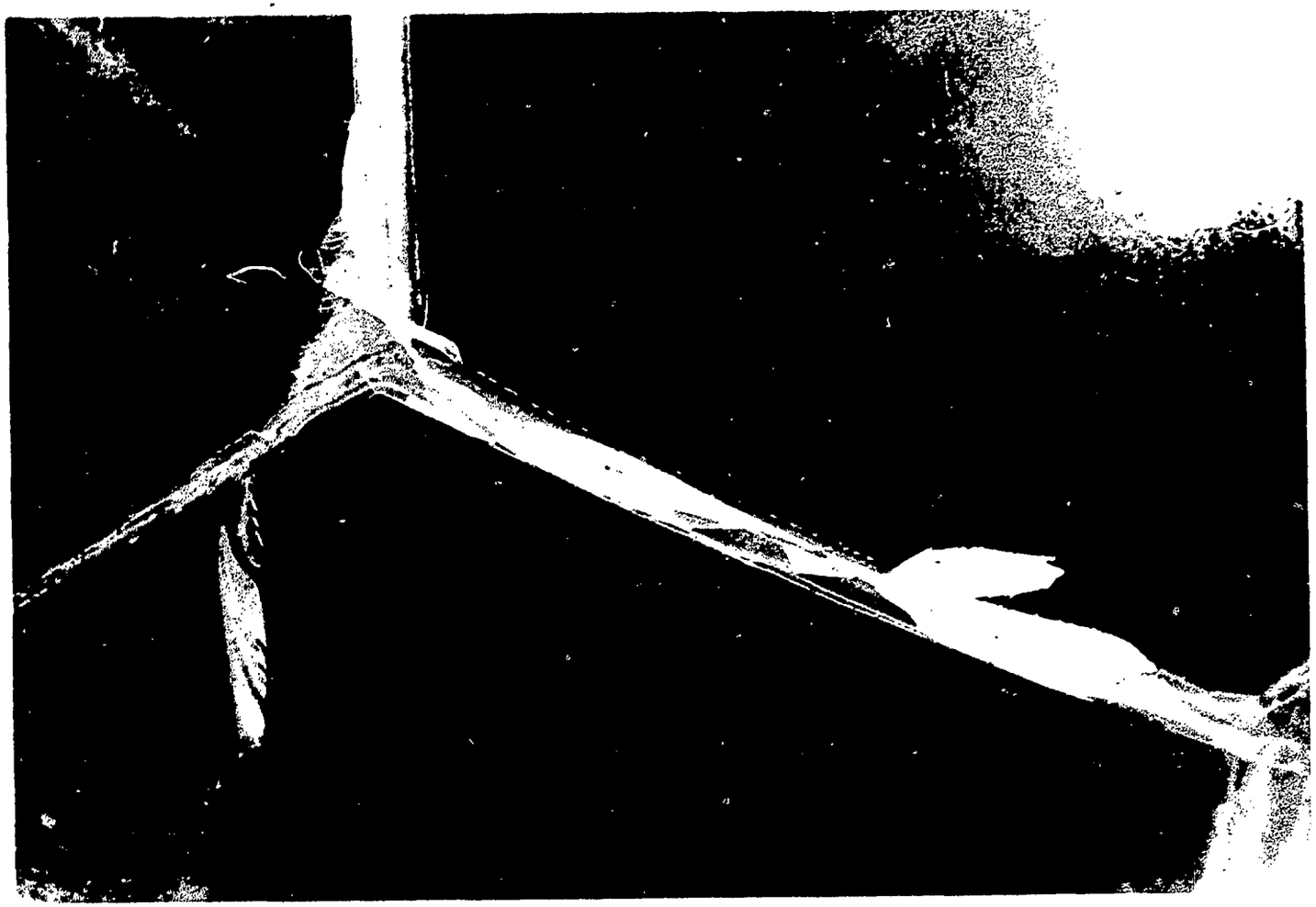

Figure 23. [illegible] capsule No. 24 after being subjected (at 1041 depth) to a 8.3 gram charge at 24 in. standoff; [illegible]

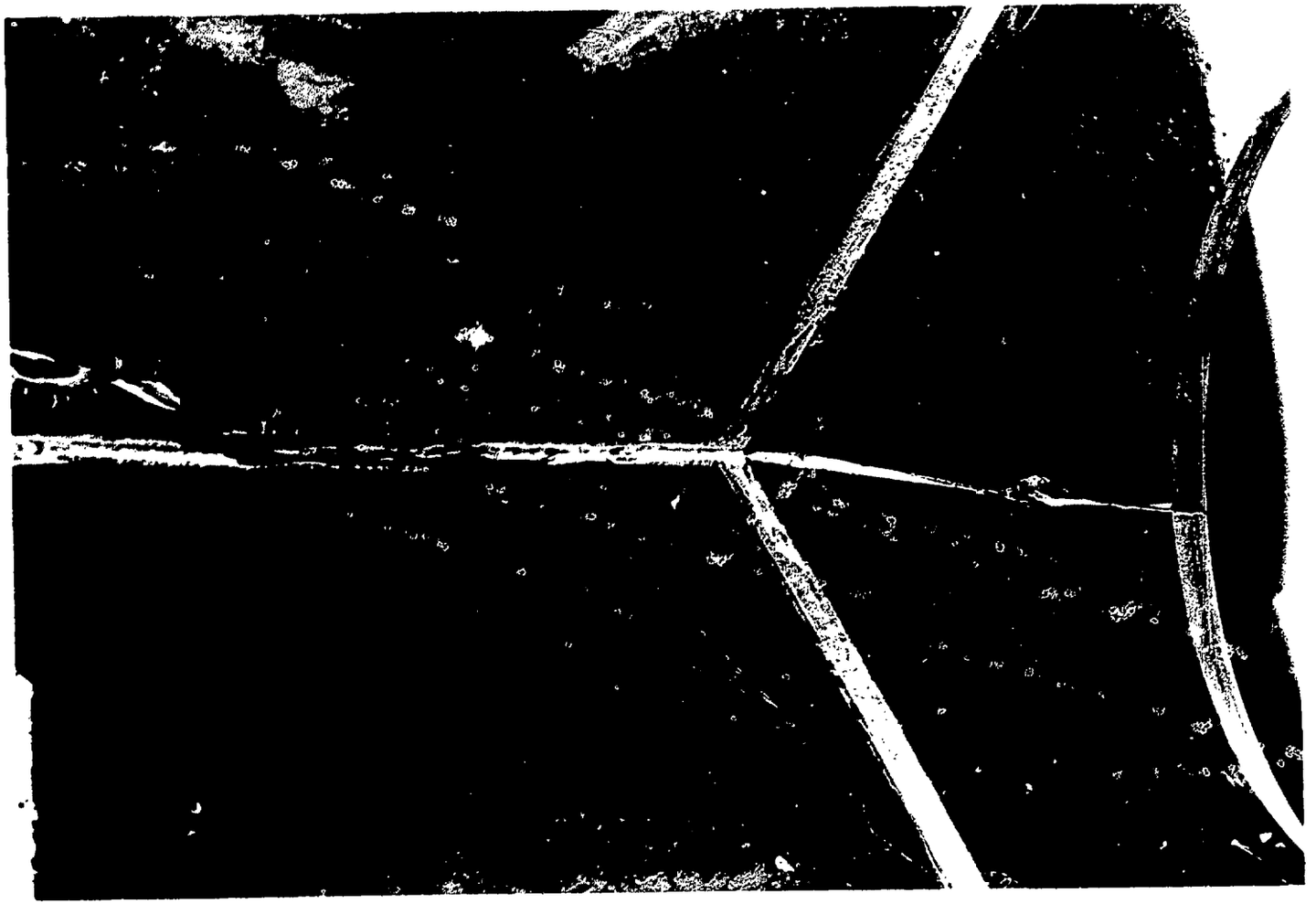

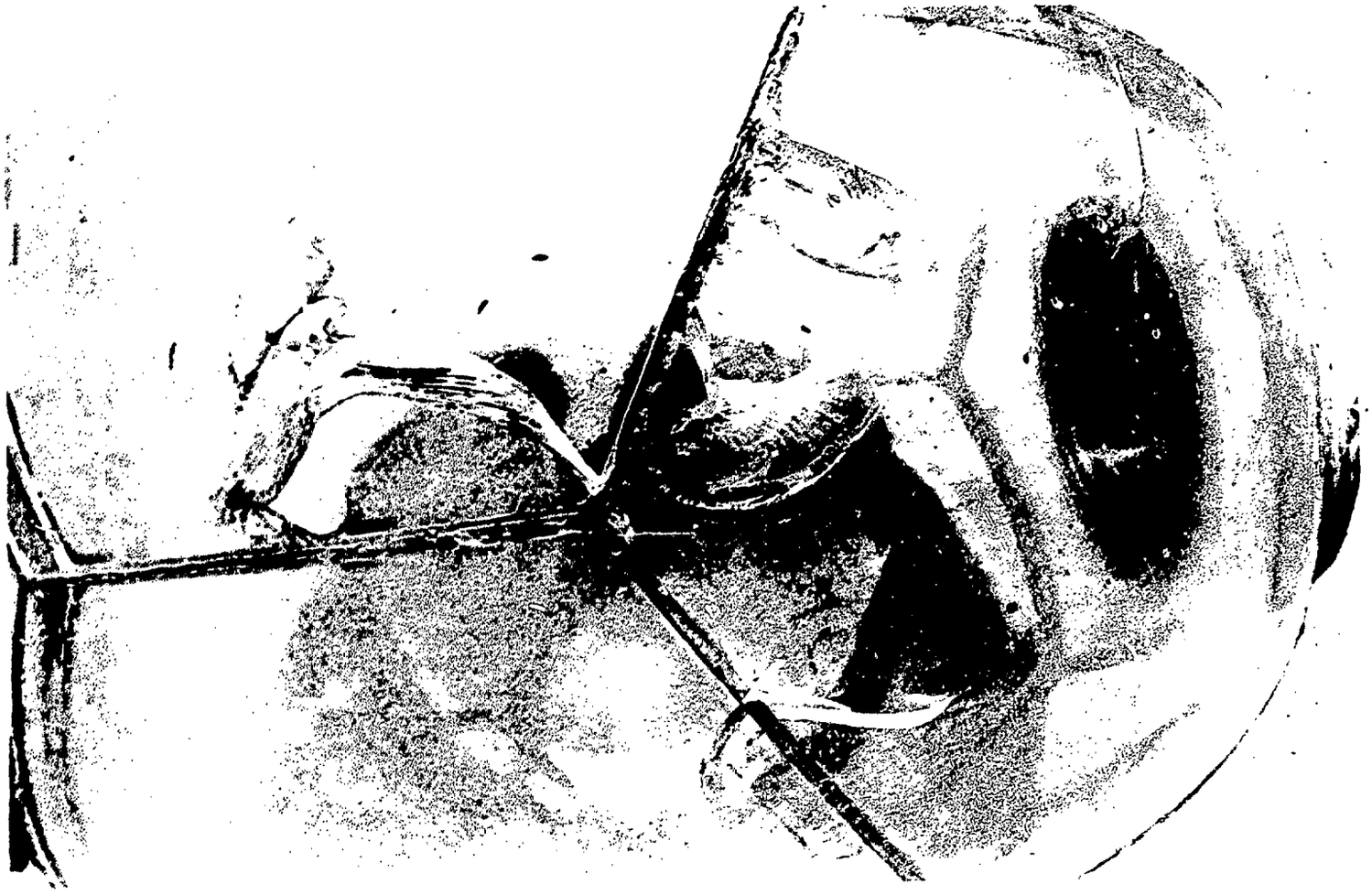

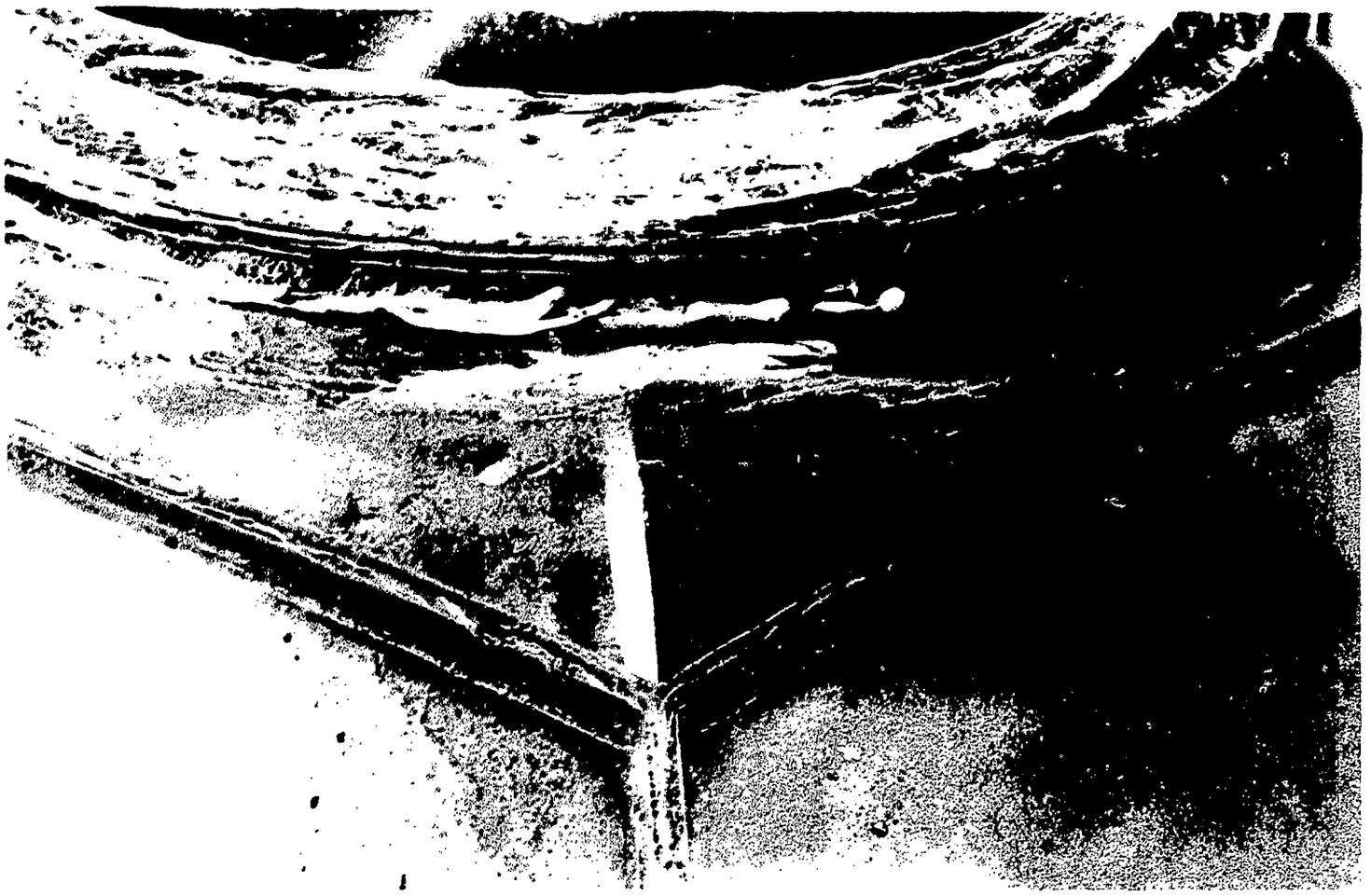

Figure 22. Fiberglass capsule No. 8, after being subjected (at 1000-ft depth) to a 14.6-gram charge at 12 in. standoff: (a) back (opposite side of capsule to explosion) (Sheet 2 of 3)

Figure 23. Fractures in capsule No. 25 after being subjected (at 10-ft depth) to a 8.2-gram charge at 48 in. standoff; view looking toward the opposite side of capsule near penetration. (Sheet 2 of 2)

Figure 24. Post-impact fracture in the M-MO Mod 2mod capsule after striking a steel beam in the test fir

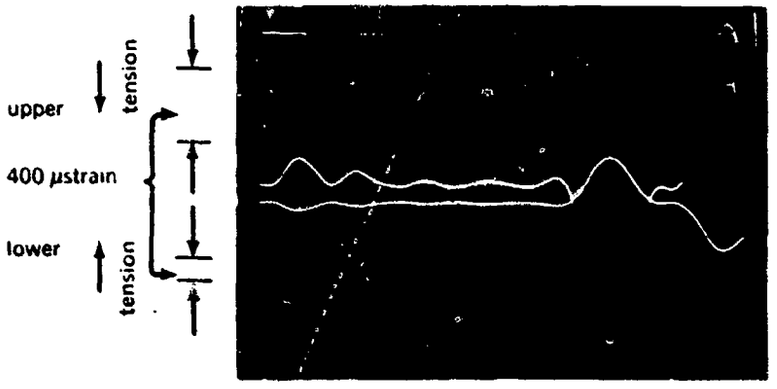

NOTES:

a) 1/4 inch strain gage was positioned internally on apex of sphere closest to point of detonation

b) Gage output was recorded at two voltage deflection levels on scope since strain level was was not known

c) 7/8 pound of pentolite was detonated 53 inches from outer surface of sphere

d) Maximum strain was initially 930 microinches in tension followed by an equal strain in compression

e) Scope trigger was delayed 10 microseconds after detonation

Figure 25. Dynamic strains measured on the interior surface of the NEMO Mod 2000 capsule directly below the charge of 387.8 grams at 52.9 in. standoff.

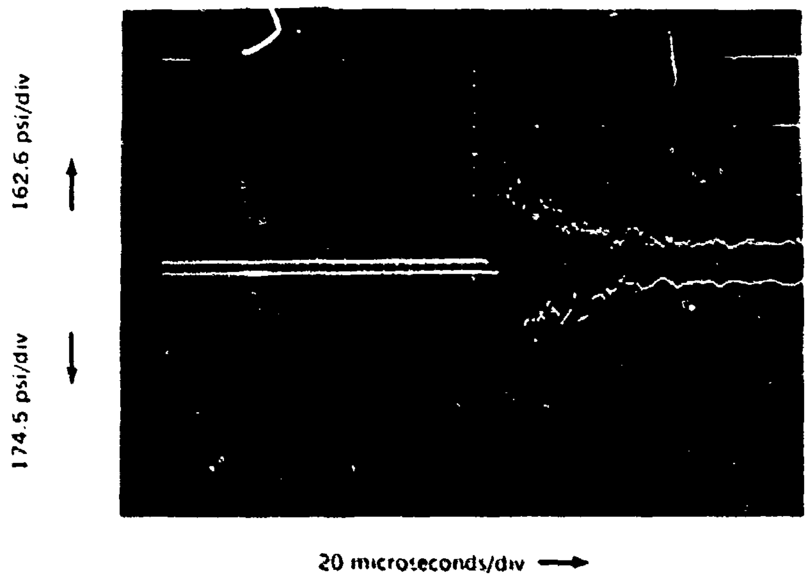

Charge:	E81 Electric Blasting Cap
Standoff:	4.41 Feet
Depth:	50 Feet
Peak Measured Pressure:	Upper Trace 504 Psi
	Lower Trace 502 Psi
Measured Unit Impulse	Not Readable
Calculated Peak Pressure	435 Psi
Calculated Unit Impulse.	.00745 Psi-Sec
Comments:	No Damage

Figure 26. Peak pressures measured at the full-size NEMO Mod 2000 capsule when the [illegible] charge was fired at 52.9 in. standoff

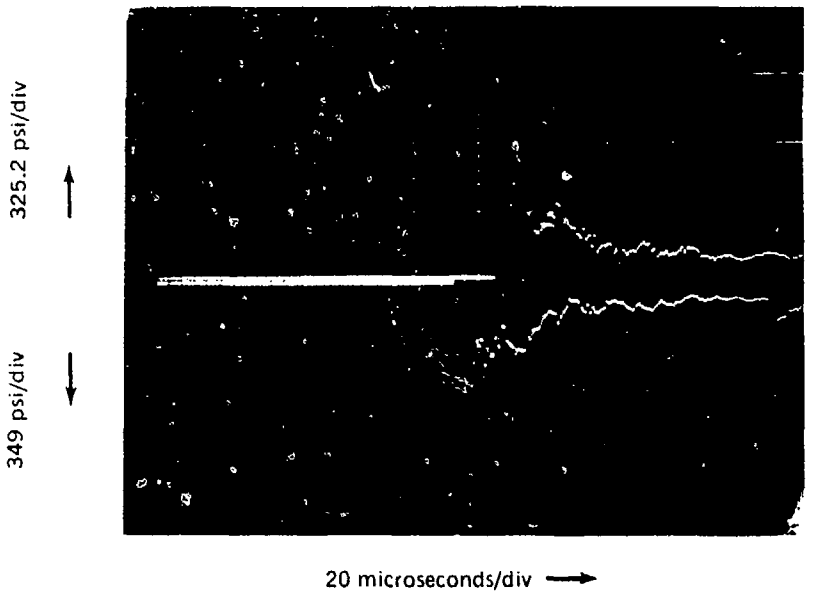

Charge:	.01242 lbs
Standoff:	4.41 Feet
Depth:	50 Feet
Peak Measured Pressure:	Upper Trace 975 Psi
	Lower Trace 1,012 Psi
Measured Unit Impulse:	Not Readable
Calculated Peak Pressure:	805 Psi
Calculated Unit Impulse:	0.0228 Psi-Sec
Comments:	Nos Damage

Figure 27. Peak pressure measured at the full-size NIMO Mod 2000 capsule when the 5.62-gram charge was fired at 52.9 in. standoff

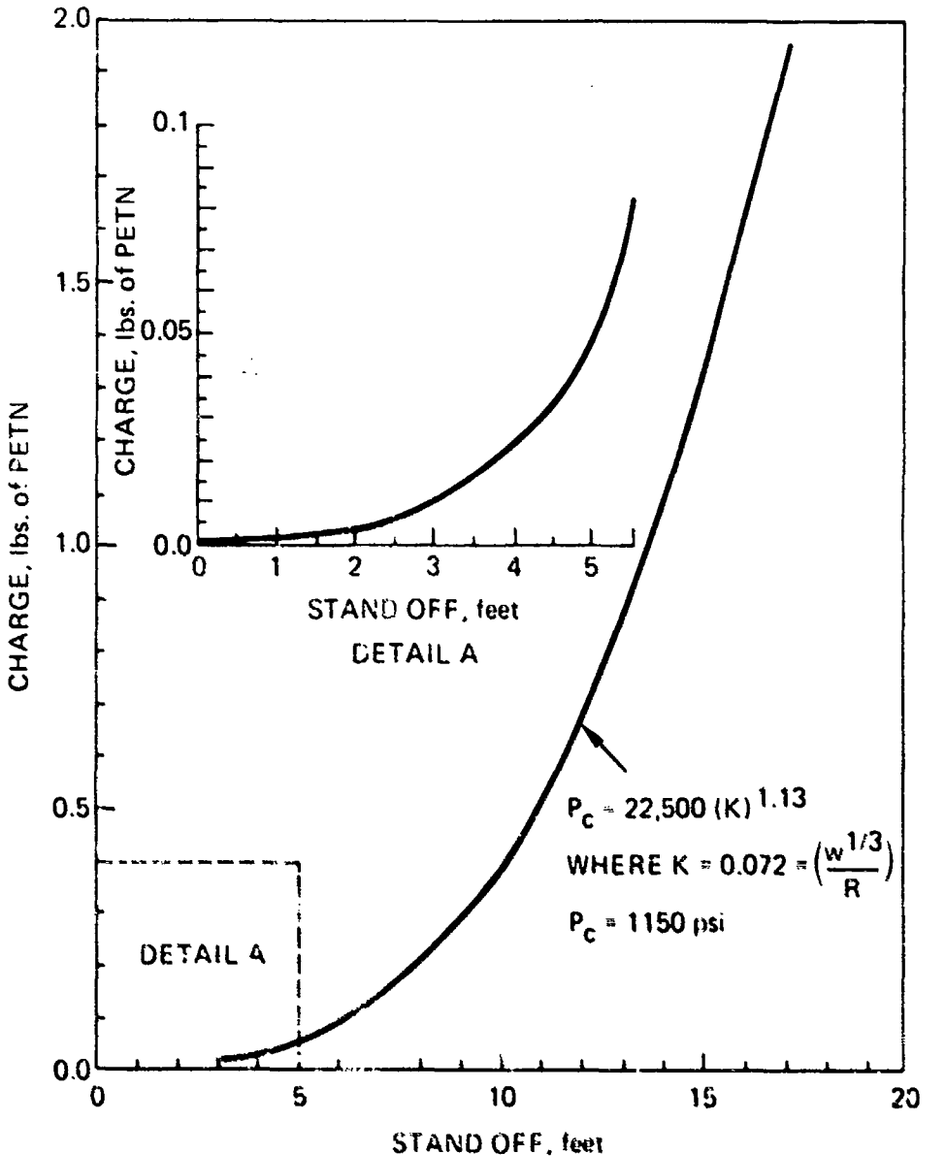

Figure 28. Weight of charge that can be repeatedly exploded underwater in the vicinity of NAVOCEANO Mod 2000 capsule without any damage to the watch, wall or its mounting in the structure of the submersible

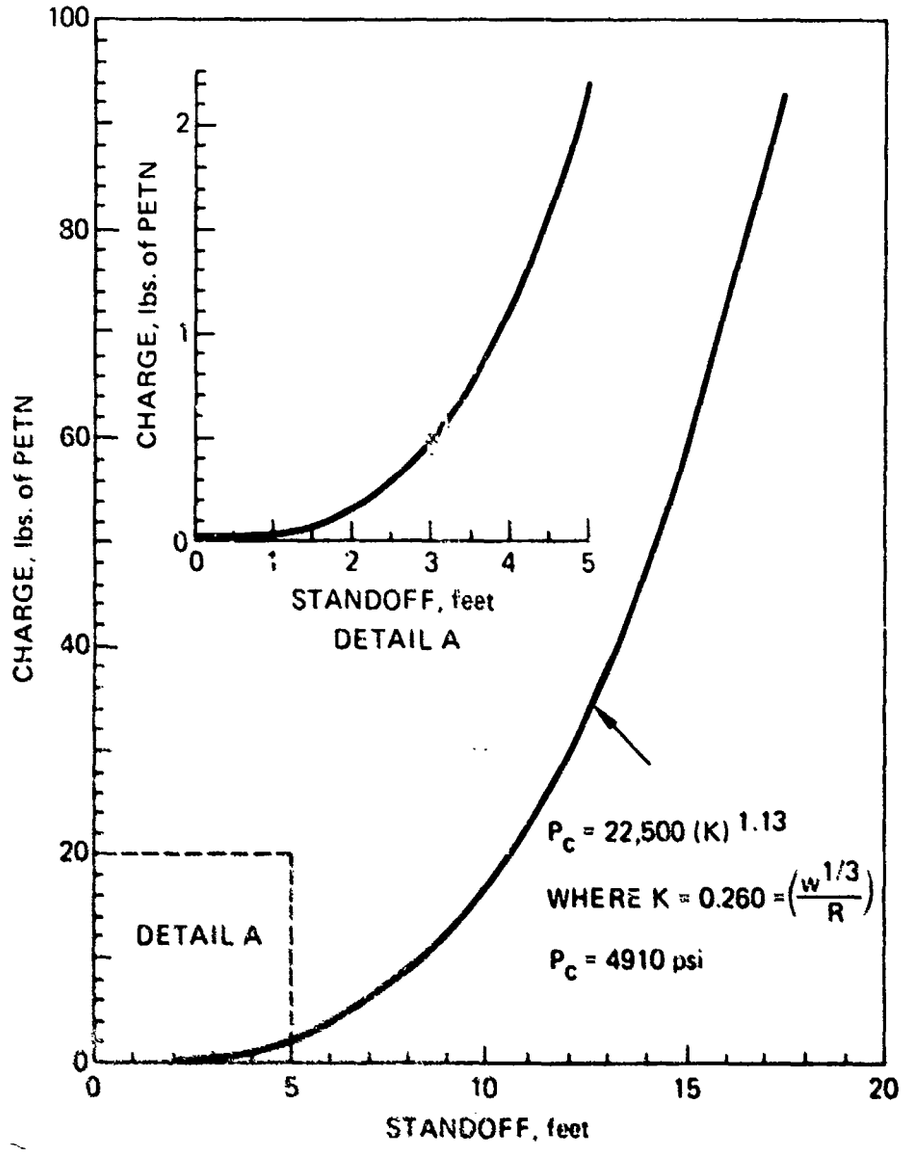

Figure 29. Maximum weight of charges that can be set off underwater in the vicinity of NEMO Mod 2000 without fracturing the hull. Such charges may, however, tear the capsule from its mounting in the structure of the submersible

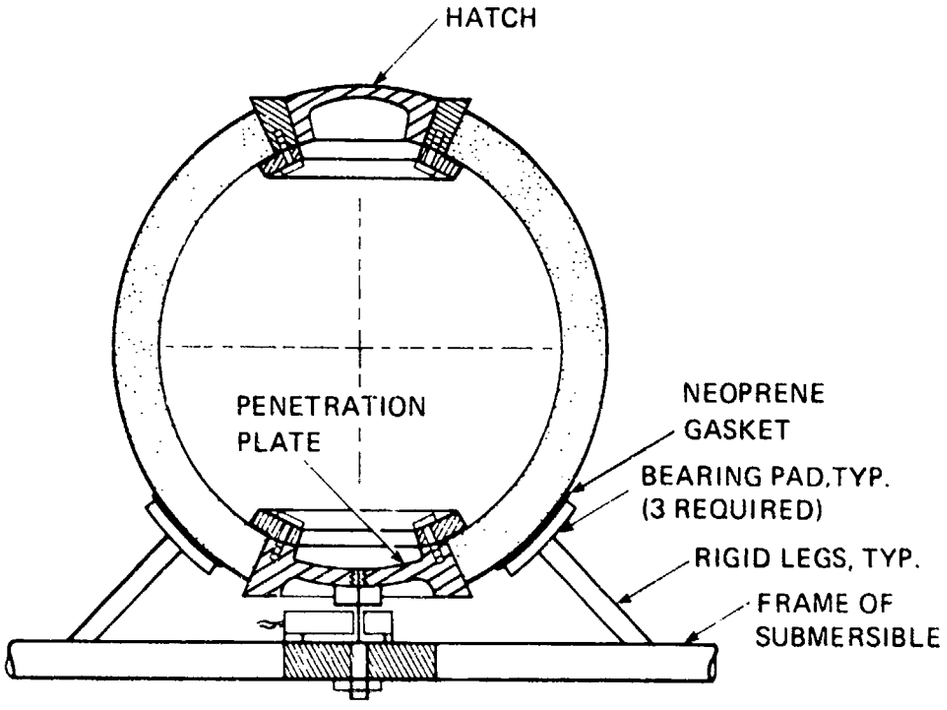

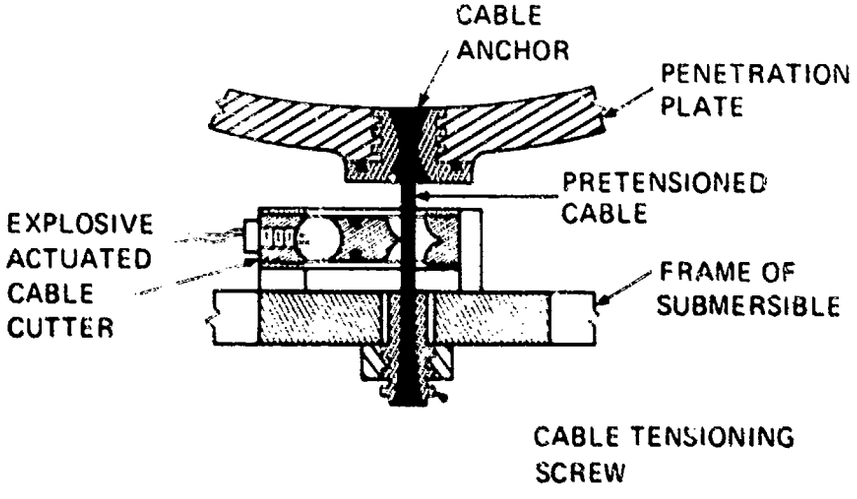

(a) SINGLE-POLE MOUNTING

Figure 30. Typical mountings for NEMO type hulls. The single-pole mounting provides better upward visibility and is very suitable for emergency release of the capsule, while the twin-pole mounting provides a more secure attachment to the frame. (Sheet 1 of 2)

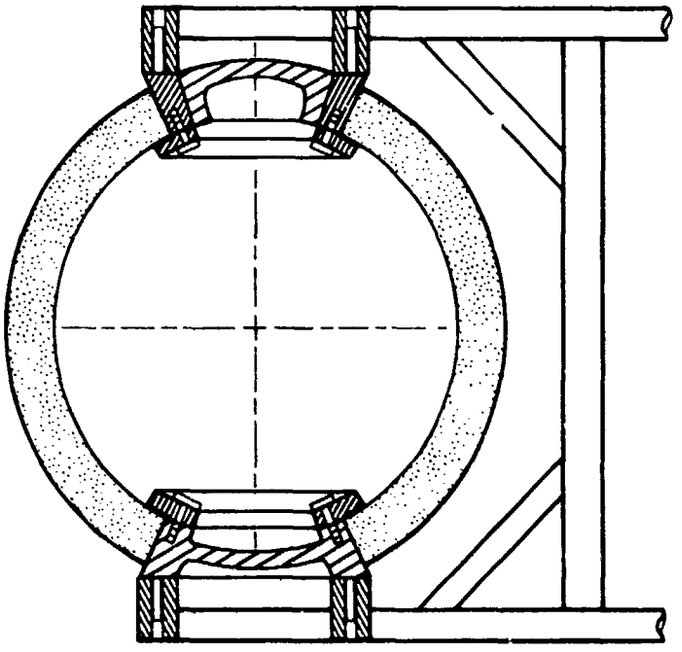

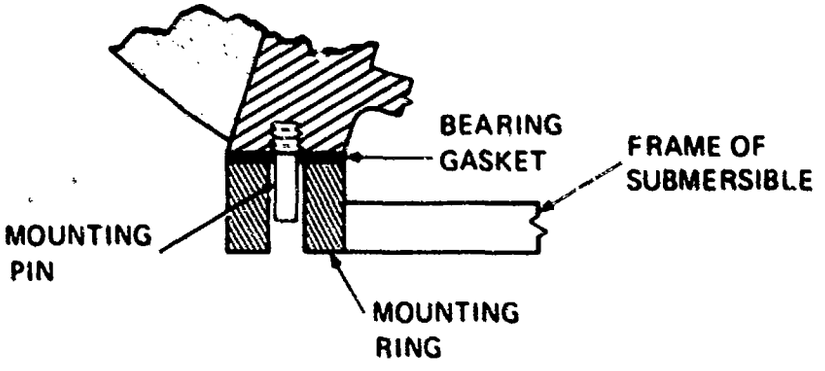

(b) TWIN-POLE MOUNTING

Figure 30. Typical mountings for NEMO type hulls. The single-pole mounting provides better upward visibility and is very suitable for emergency release of the capsule, while the twin-pole mounting provides a more secure attachment to the frame. (Sheet 2 of 2)

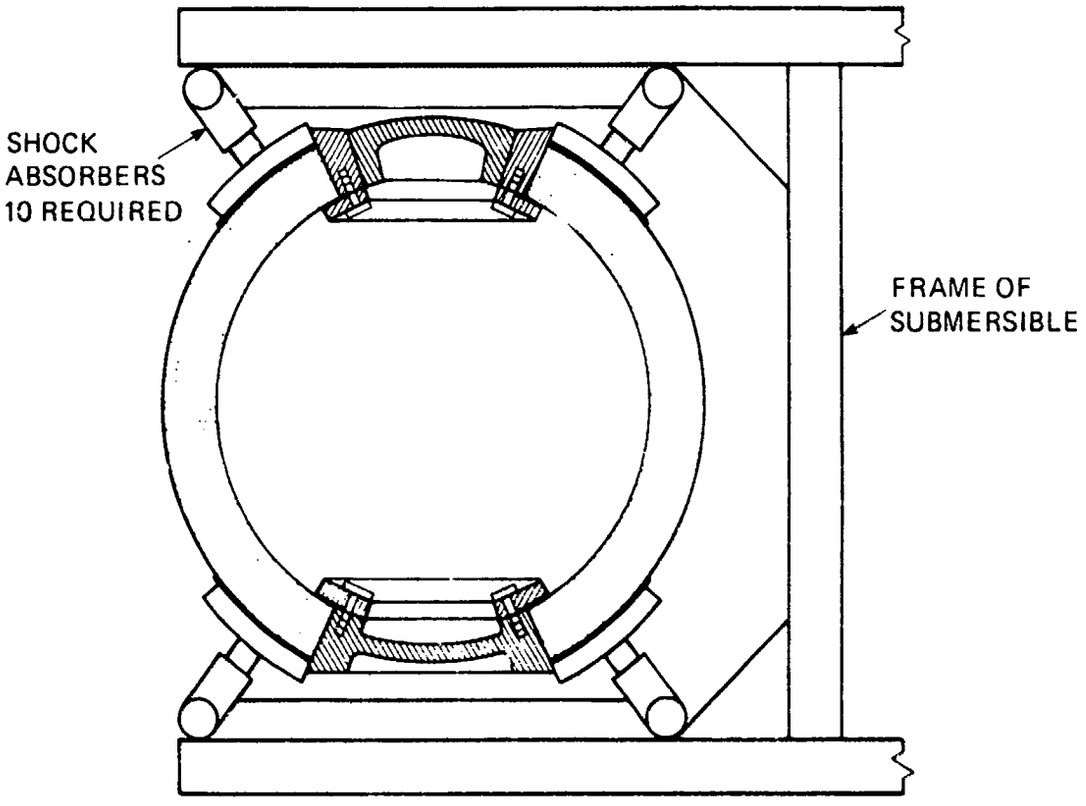

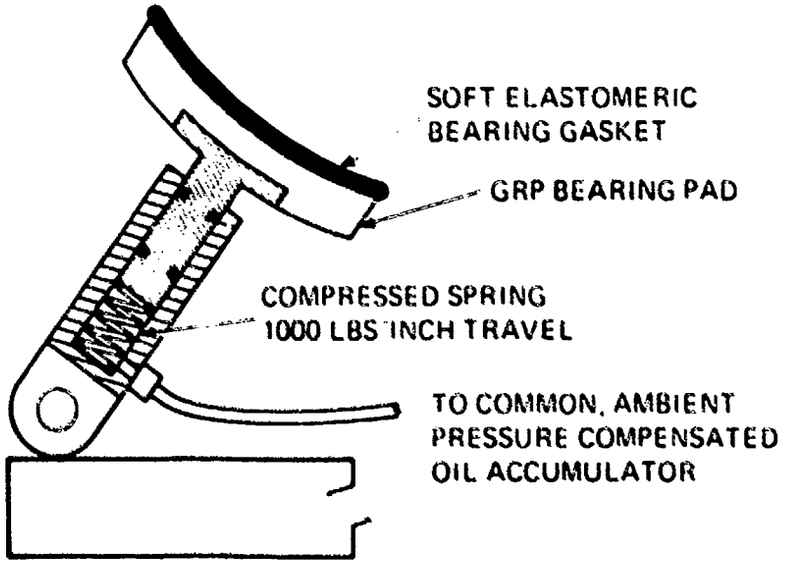

Figure 31 Concept of a mounting providing acoustic, but shock-mitigating attachment to the frame

APPENDIX

DESCRIPTION OF TEST SPECIMENS

MODEL J

Outside diameter:		15 in.
Inside diameter:		13 in.
Shell thickness:		0.040 - 0.980 in.
Material:		Plexiglas G
Construction:		Assembly of 12 thermoformed pentagons bonded with PS-30 adhesive (Fig. 3).
Penetrations:	top	5.285 in. minor diameter with 48° included angle
	bottom	4.445 in. minor diameter with 40° included angle
Inserts:	top	Type B (Fig. 4), 6A14V titanium
	bottom	Type A (Fig. 4), 6A14V titanium
Insert gasket:	top	polycarbonate gasket (Fig. 4)
	bottom	none
Life history:		Pressure cycled 1000 times to 1000 psi in tap water at 61-74°F ambient temperature. Typical pressure cycle consisted of pressurizing to 1000 psi, holding at 1000 psi for 4 hours, depressurizing to 0 psi, and relaxing for 4 hours at 0 psi.

MODEL K

Outside diameter:	15 in.
Inside diameter:	13 in.
Shell thickness:	0.935 – 0.975 in.
Material:	Plexiglas G
Construction:	Assembly of 12 thermoformed pentagons bonded with PS-30 adhesive (Fig. 3)
Penetrations: top	– 5.285 in. minor diameter with 48° included angle
bottom	– 4.445 in. minor diameter with 40° included angle
Inserts: top	– Type B (Fig. 4) 6A14V titanium
bottom	– Type A (Fig. 4) 6A14V titanium
Insert gasket: top	– polycarbonate gasket (Fig. 4)
bottom	– none
Life history:	– Pressure cycled 1000 times to 1500 psi in tap water at 61-74°F ambient temperature. Typical pressure cycle consisted of pressurizing to 1500 psi, holding at 1500 psi for 4 hours, depressurizing to 0 psi, and relaxing for 4 hours at 0 psi.

MODEL M

Outside diameter:		15 in.
Inside diameter:		13 in.
Shell thickness:		0.930 0.990
Material:		Plexiglas G
Construction:		Assembly of 12 thermoformed pentagons bonded with PS-30 adhesive (Fig. 3)
Penetrations:	top	5.285 in., minor diameter with 48° included angle
	bottom	4.445 in., minor diameter with 40° included angle
Inserts:	top	Type B (Fig. 4), 6A14V titanium
	bottom	Type A (Fig. 4), 6A14V titanium
Insert gasket:	top	polycarbonate gasket (Fig. 4)
	bottom	none
Life history:		Pressure cycled 1050 times to 500 psi in tap water at 61-74° F ambient temperature. Typical pressure cycle consisted of pressurizing to 500 psi, holding at 500 psi for 4 hours, depressurizing to 0 psi, and relaxing for 4 hours at 0 psi

MODEL 24

Outside diameter:	15 in.
Inside diameter:	14 in.
Shell thickness:	0.460 – 0.490 in.
Material:	Plexiglas G
Construction:	Assembly of 12 thermoformed pentagons bonded with PS-18 adhesive (Fig. 5).
Penetrations:	top – 4.793 in., minor diameter with 40° included angle bottom – 4.793 in., minor diameter with 40° included angle
Inserts:	top – Type C (Fig. 6), 316 stainless steel bottom – Type C (Fig. 6), 316 stainless steel
Insert gasket:	top – none bottom – none
Life history:	– Pressure cycled 1056 times to 500 psi in tap water at 61-74°F ambient temperature. Typical pressure cycle consisted of pressurizing to 500 psi, holding at 500 psi for 4 hours, depressurizing to 0 psi, and relaxing for 4 hours at 0 psi.

MODEL 25

Outside diameter:		15 in.
Inside diameter:		14 in.
Shell thickness:		0.460 - 0.490 in.
Material:		Plexiglas G
Construction:		Assembly of 12 thermoformed pentagons bonded with PS-18 adhesive (Fig. 5).
Penetrations:	top	5.150 in., minor diameter with 43° included angle
	bottom	5.150 in., minor diameter with 43° included angle
Inserts:	top	Type C (Fig. 6), 316 stainless steel
	bottom	Spherical shell sector, 0.5 in. thick with 43° included angle, acrylic plastic
Insert gasket:	top	polycarbonate gasket, (Fig. 6)
	bottom	none
Life history:		Pressure cycled 1056 times to 500 psi in tap water at 61-74°F ambient temperature. Typical pressure cycle consisted of pressurizing to 500 psi, holding at 500 psi for 4 hours, depressurizing to 0 psi, and relaxing for 4 hours at 0 psi.

MODEL 26

Outside diameter:		15 in.
Inside diameter:		14 in.
Shell thickness:		0.460 – 0.500 in.
Material:		Plexiglas G
Construction:		Assembly of 12 thermoformed pentagons bonded with PS-18 adhesive (Fig. 5)
Penetrations:	top	– 5.150 in., minor diameter with 43° included angle
	bottom	– none
Inserts:	top	– Spherical shell sector, 0.5 in. thick with 43° included angle, acrylic plastic
	bottom	– none
Insert gasket:	top	– none
	bottom	– none
Life history:		– Was not subjected to any hydrostatic tests prior to explosive testing.

MODEL NEMO 2000

Outside diameter:		66 in.
Inside diameter:		57.900 in.
Shell thickness:		4.050 in.
Material:		Plexiglass G
Construction:		Assembly of 12 thermoformed pentagons bonded with PS-30 adhesive (Fig. 7).
Penetrations:	top	23.822 in., minor diameter with 48°30′ included angle
	bottom	21.727 in., minor diameter with 44° included angle
Inserts:	top	Working hatch, 6061-T6 aluminum (Appendix A)
	bottom	penetration plate, 6061-T6 aluminum (Appendix A)
Insert gasket:	top	polycarbonate gasket (Appendix A)
	bottom	polycarbonate gasket (Appendix A)
Life history:		Pressure cycled one time each to 450 psi, 900 psi, 1350 psi, and 1800 psi. Each pressure cycle consisted of pressurizing to maximum pressure, holding at that pressure for 24 hours, depressurizing to 0 psi, and relaxing for 24 hours at 0 psi.

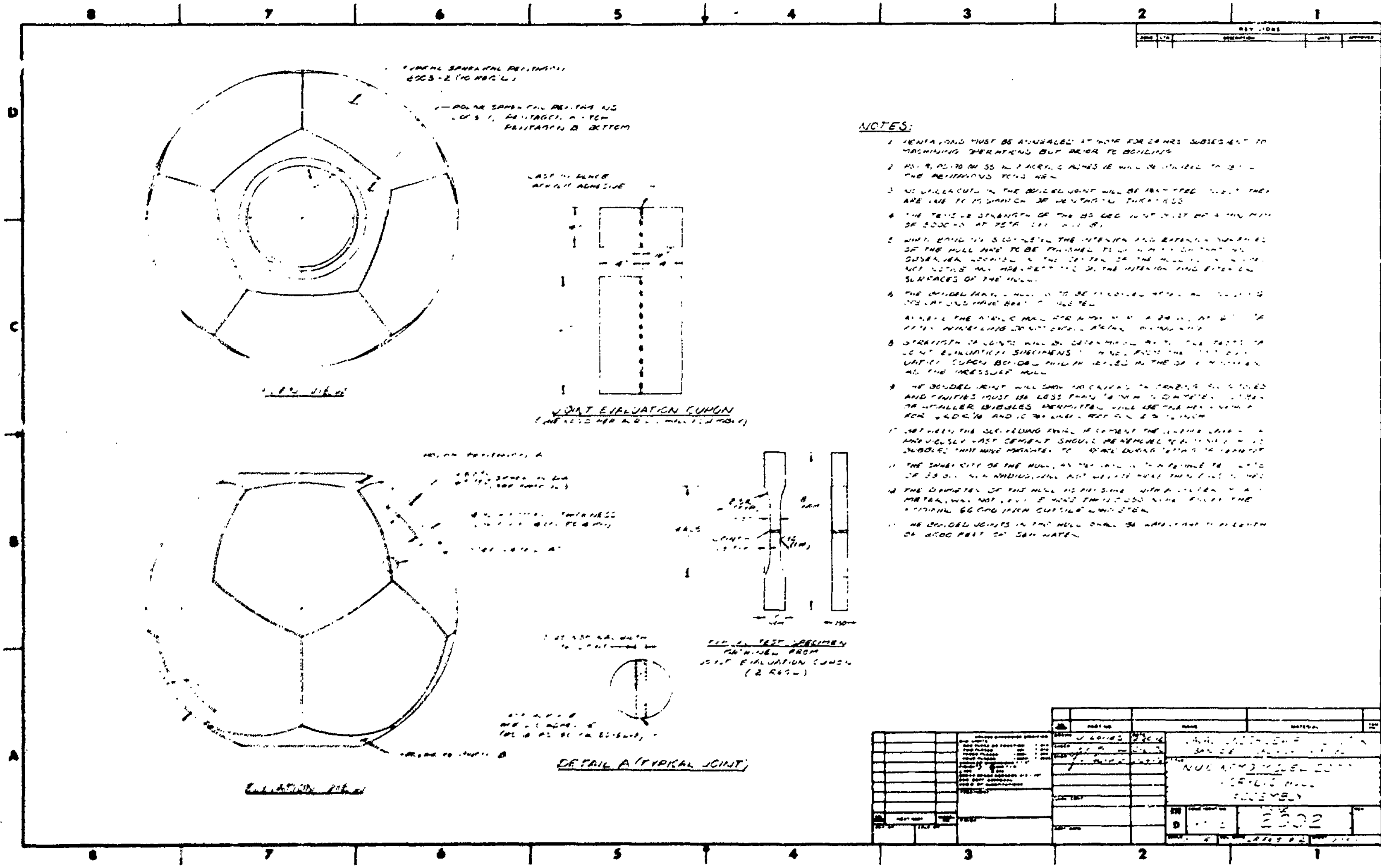
NOTES:
JOINT EVALUATION COUPON
DETAIL A (TYPICAL JOINT)

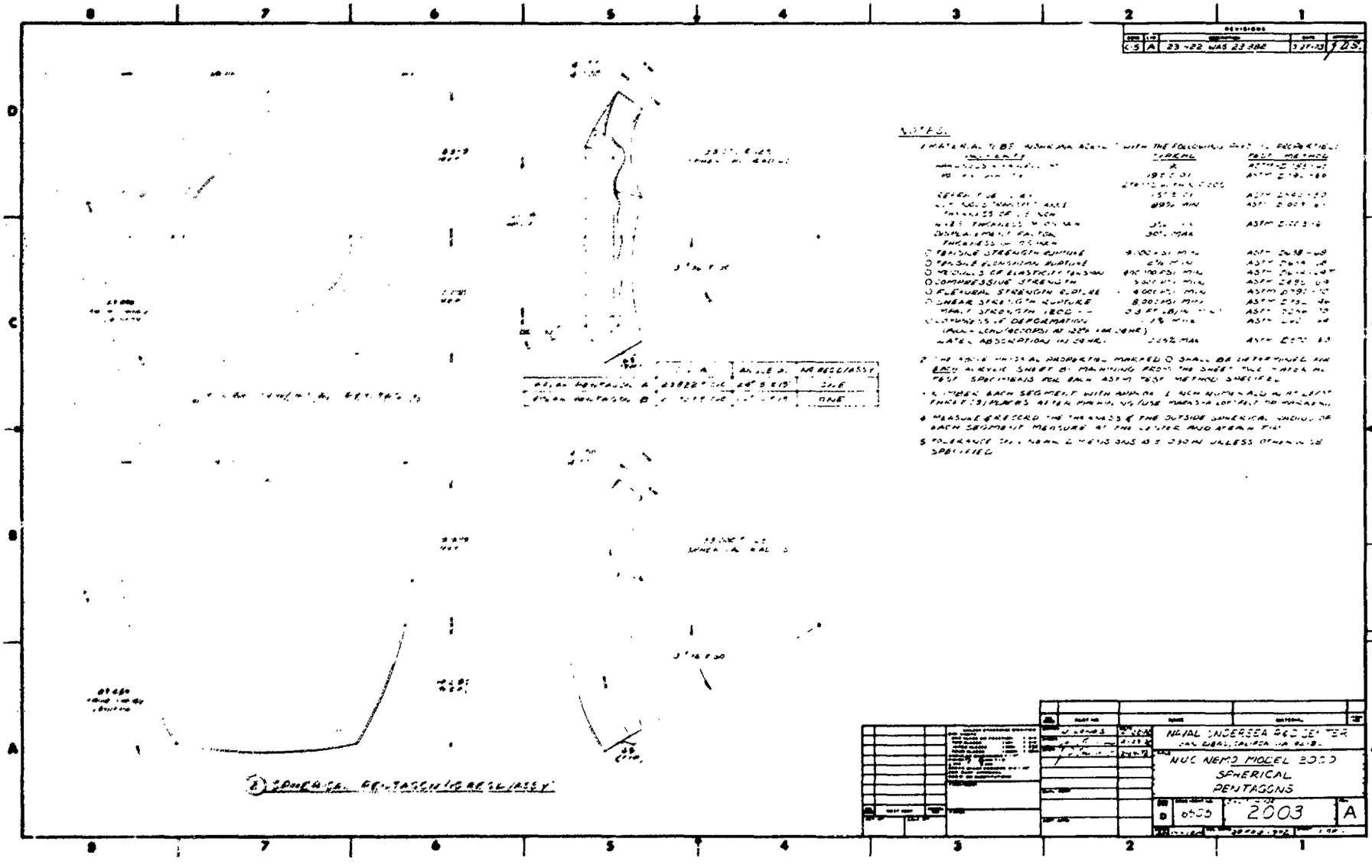

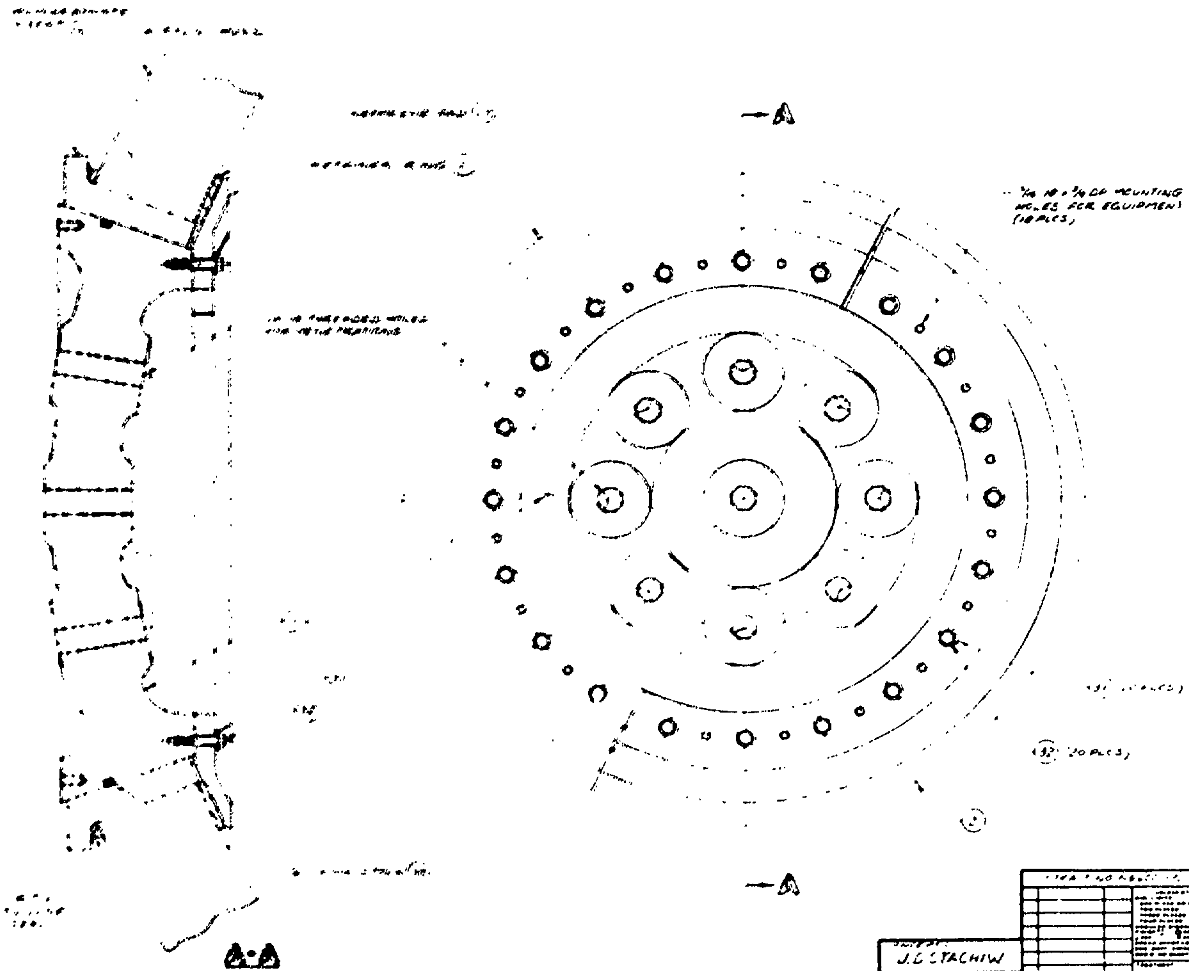

1	3/8 DIA × 1 1/4	PN: MS17987-613	STEEL	46
3	SSN-5PN	BALL PLUNGER	VLIER ENG CORP.	45
9	1/4 I.D.	WASHER	18-8 STAINLESS	44
3	1/4-20 × 5/8	SOCKET HD SCREW	" "	43
6	1/2-12 × 1 3/8	" " "	" "	42
6	5/16-18 × 7/8	" " "	" "	41
2	1/4-20 × 2 1/4	" " "	" "	40
12	3/8-16 × 7/8	" " "	" "	39
6	#10-24 × 1/2	" " "	" "	38
3	5/8-18 NUT	FINISHED FULL	" "	37
3	5/8-18 NUT	MS35692-1030	" "	36
9	1/4-20 × 3/4	SOCKET HD SCREW	" "	35
3	C0360-045-0500S	LATCH BUTTON SPRING	ASSOC. SPRING CORP.	34
6	3/32 DIA × 1 1/4	ROLL PIN	DRIV-LOK #SS-156-1250	33
40	5/16-18 × 1 1/2	HEX. HEAD BOLT	18-8 STAINLESS	32
40	5/16 I.D.	WASHER	" "	31
20'	1/4 SECTION	O-RING STOCK	BUTYL	30
6	#2-14	O-RING 1/2 I.D. × 1/16 W	NITRILE (BUNA N)	29
3	2011-5	LIFTING EYE	4340 STEEL	28
2	2011-4	BOTTOM RETAINER PAD	60 DUR NEOPRENE	27
2	2011-3	TOP RETAINER PAD	"	26
1	2011-2	BOTTOM INSERT	[illegible] 3030 UV RESIST	25
1	2011-1	TOP INSERT	"	24
1	2010-3	SPRING #AS42016	ASSOC. SPRING CORP.	23
1	2010-2	SPRING #AS41878	" " "	22
2	2010-1	TOP RETAINER RING	6061-T6 ALUM	21
1	2009-6	HINGE PIN	17-4PH STAINLESS	20
1	2009-5	SPRING RETAINER	6061-T6 ALUM	19
2	2009-4	BUMPER PAD	60 DUR NEOPRENE	18
2	2009-3	HINGE BUSHING	17-4PH STAINLESS	17
1	2009-2	RIGHT HATCH HINGE	6061-T6 ALUM	16
1	2009-1	LEFT HATCH HINGE	" " "	15
1	2008-3	HINGE PLATE	" " "	14
1	2008-2	RIGHT STA. HINGE	" " "	13
1	2008-1	LEFT STA. HINGE	" " "	12
3	2007-8	INTERIOR HANDLE	" " "	11
3	2007-7	EXTERIOR HANDLE	" " "	10
3	2007-6	LATCH LUG	17-4PH STAINLESS	9
3	2007-5	STRIKER PLATE	" "	8
3	2007-4	LATCH BUTTON	6061-T6 ALUM	7
6	2007-3	THRUST WASHER	303 STAINLESS	6
3	2007-2	LATCH SHAFT	[illegible]	5
1	2007-1	HATCH	6061-T6 AL FORGING	4
1	2006	HATCH RING	" " " "	3
2	2005-2	BOTTOM RETAINER RING	"	2
	2005-1	BOTTOM PLATE	" "	1

NAVAL UNDERSEA R & D CENTER

N.U.C. NEMO MODEL 2000
BOTTOM PLATE
ASSEMBLY

D 65C5 2004

J. D. STACHIW

J. JONES

REMOTE ENGINEERING

... to DDC does not
... reproduction

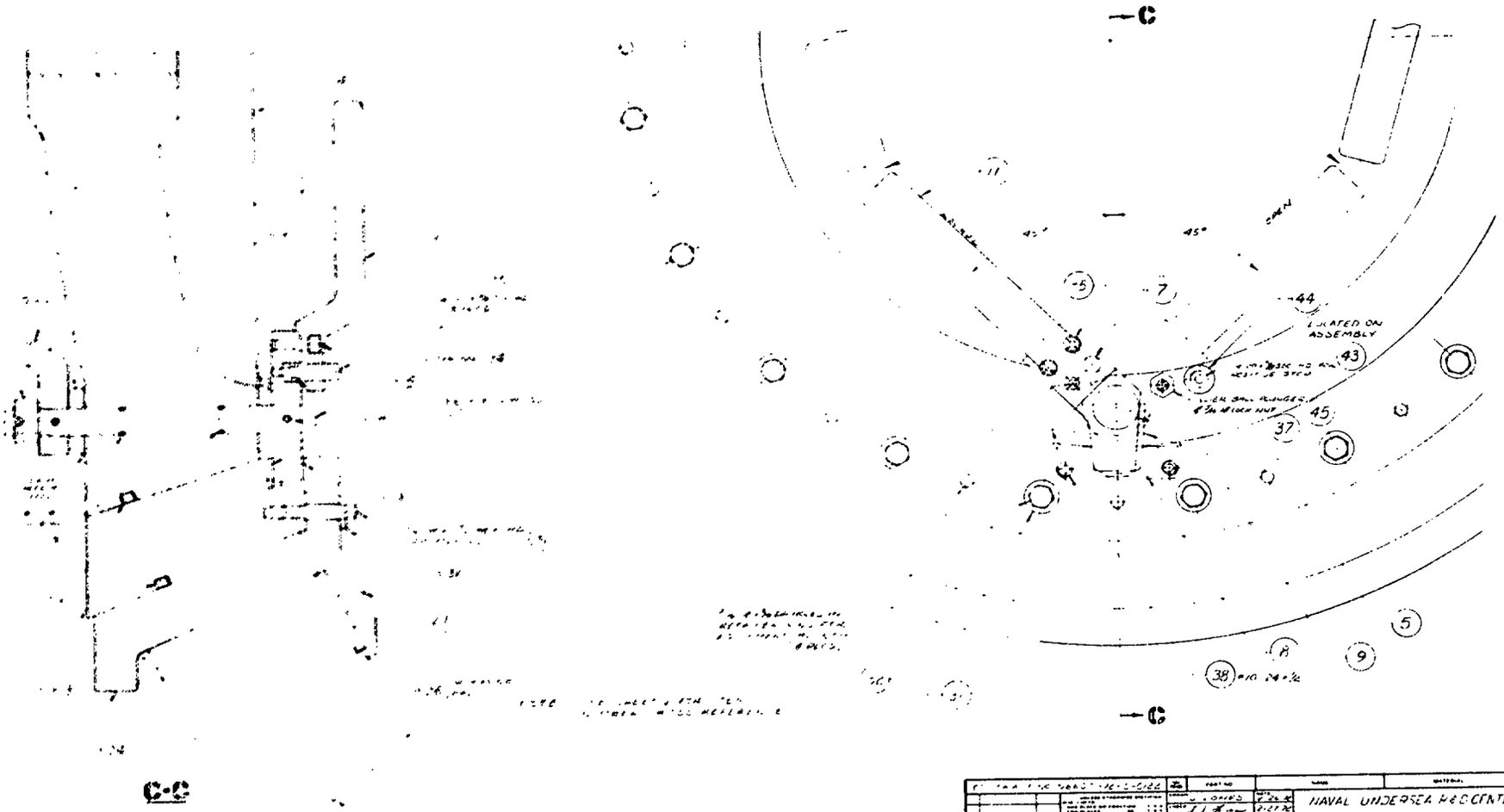

D STACHIW	NAVAL UNDERSEA R&D CENTER	
J LINES	N. U. NEMO MODEL 2000	
	HATCH LOCK ASSEMBLY	
	D 5505	2004

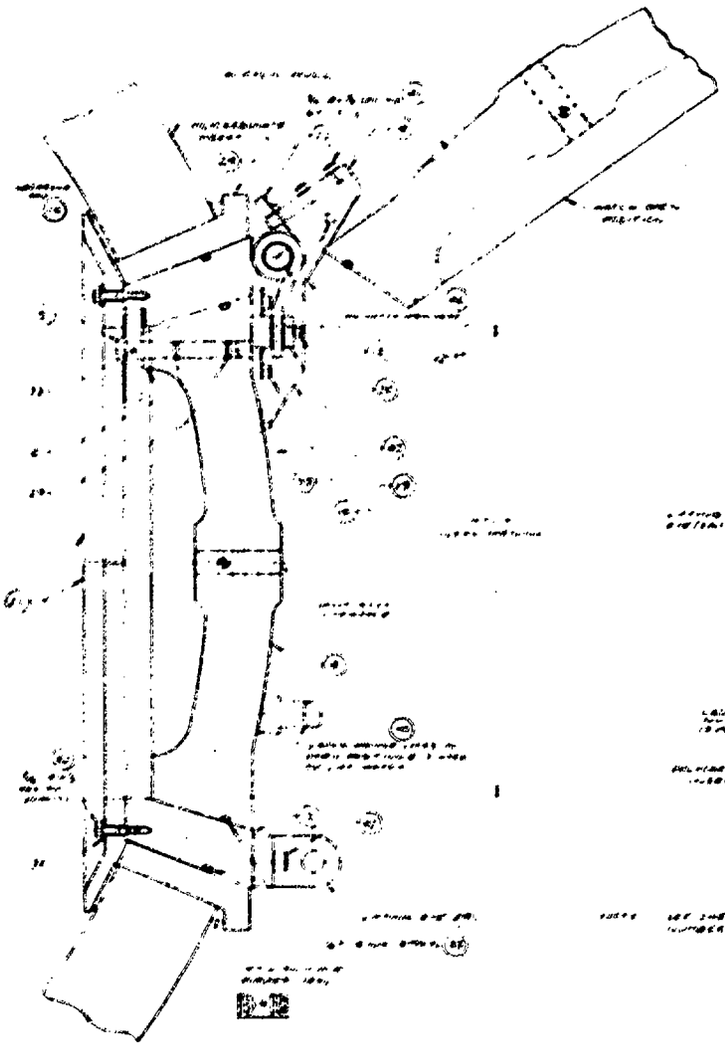

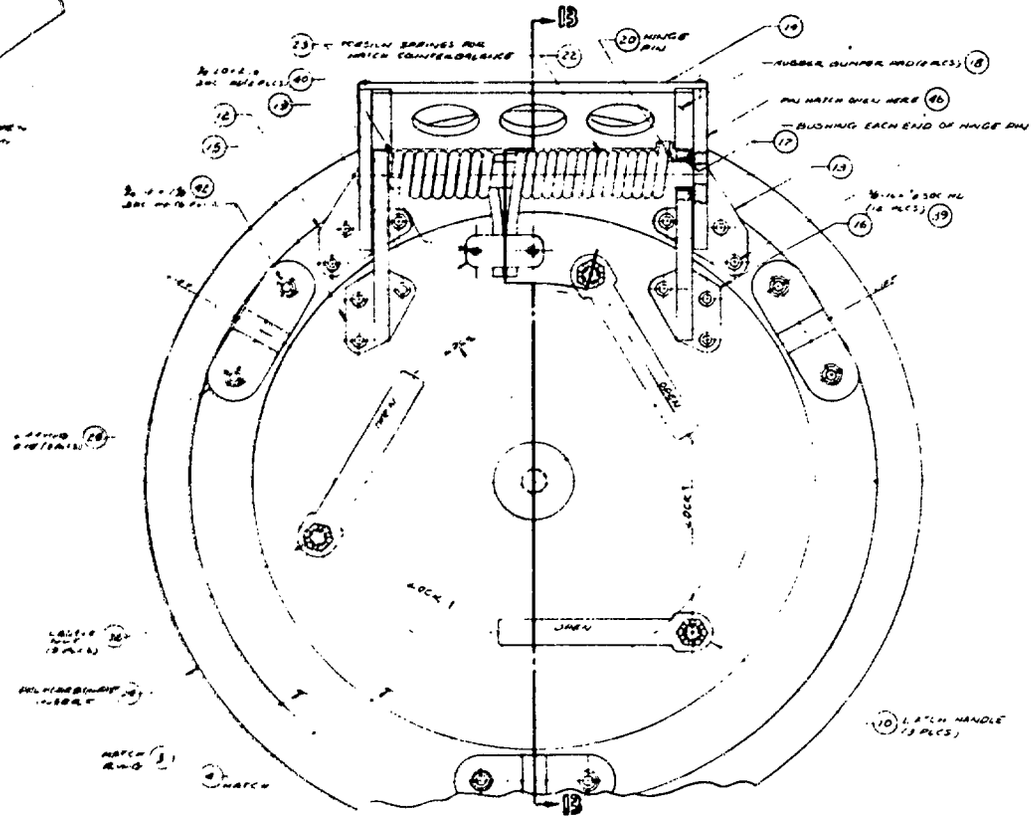

DRAWN J. JONES 2-26-72		NAVAL UNDERSEA R.&D. CENTER	
CHECKED J. D. Stalnaker 2-27-72		NUC. NEMO MODEL 2000	
ENGINEER J. D. Stalnaker 2-24-72		HATCH ASSEMBLY	
APPROVED J.C. STACH III		SIZE D	DRAWING NO. 6505 2004
CHECKED J. JONES		SCALE	DATED FEB 1972 SHEET 2 OF 3
RELEASED BY NAVY ENGINEER N/A			

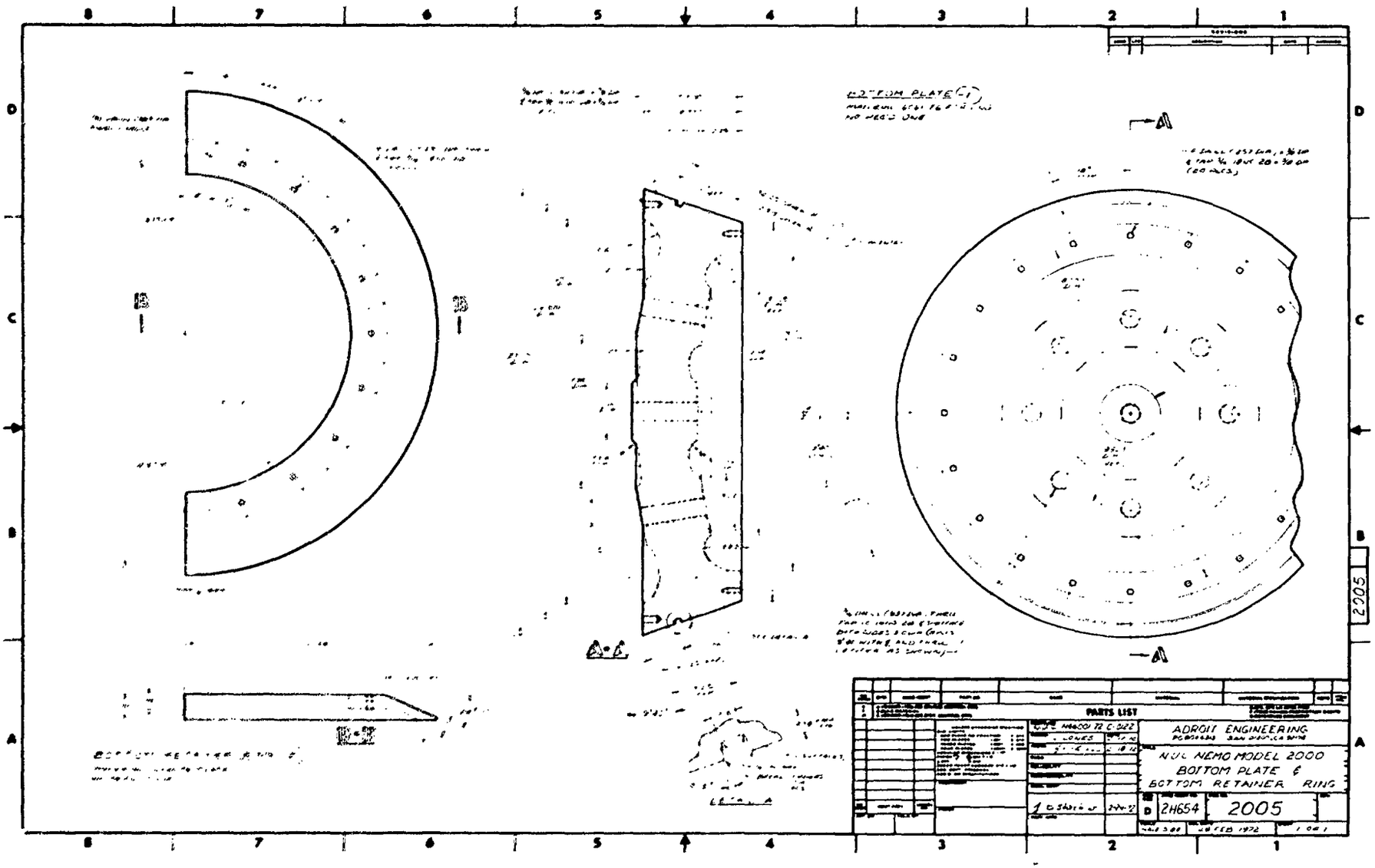

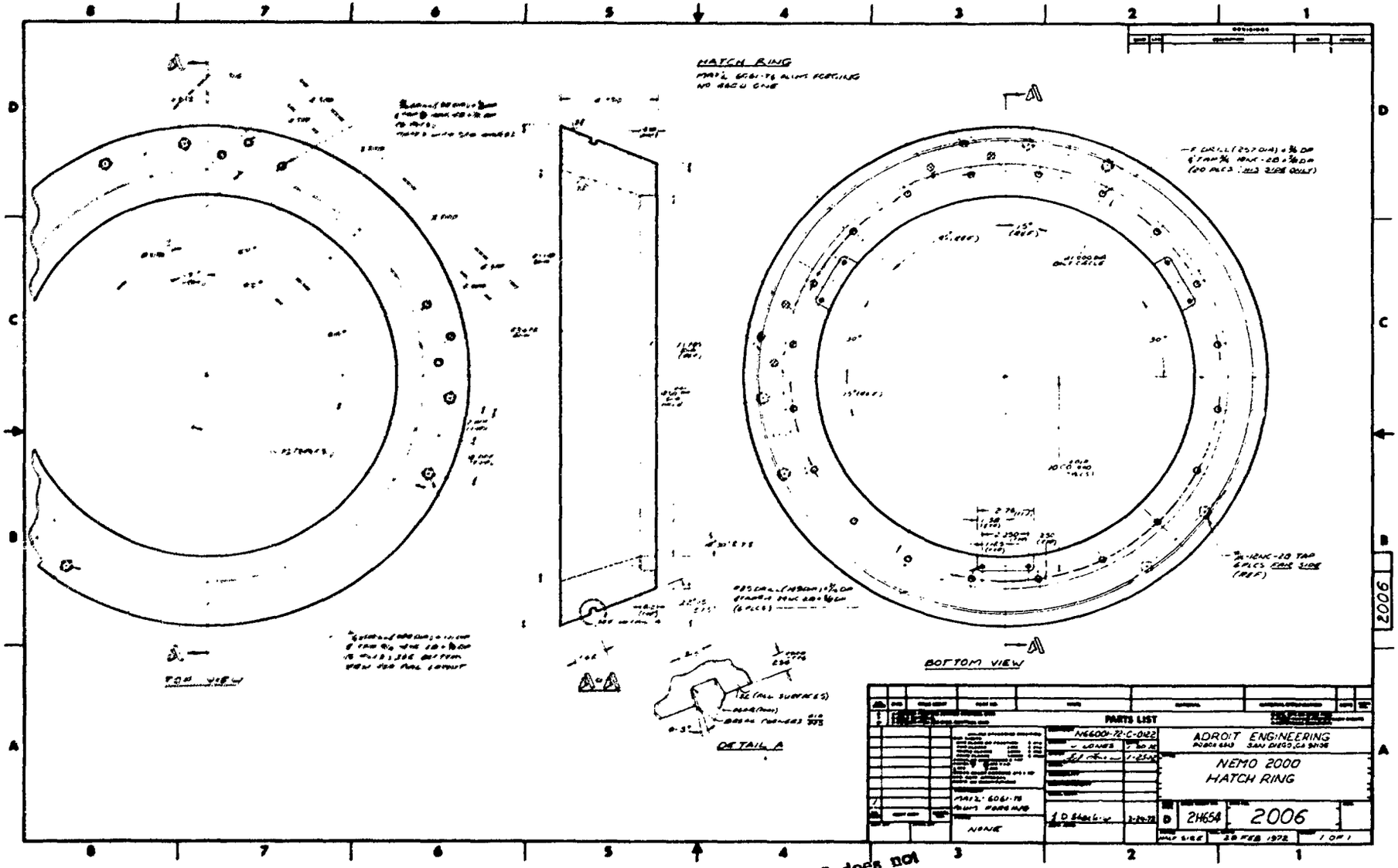

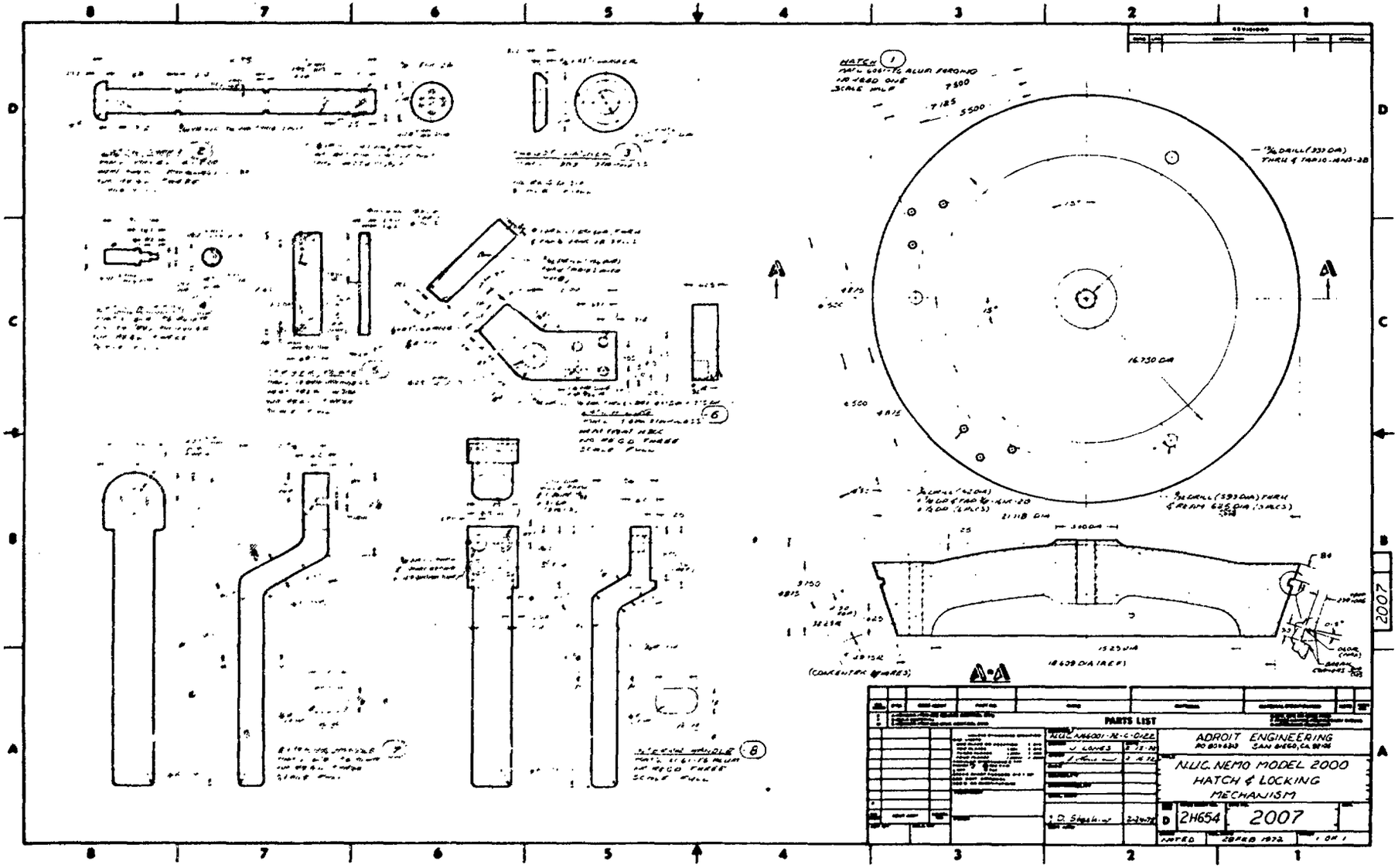

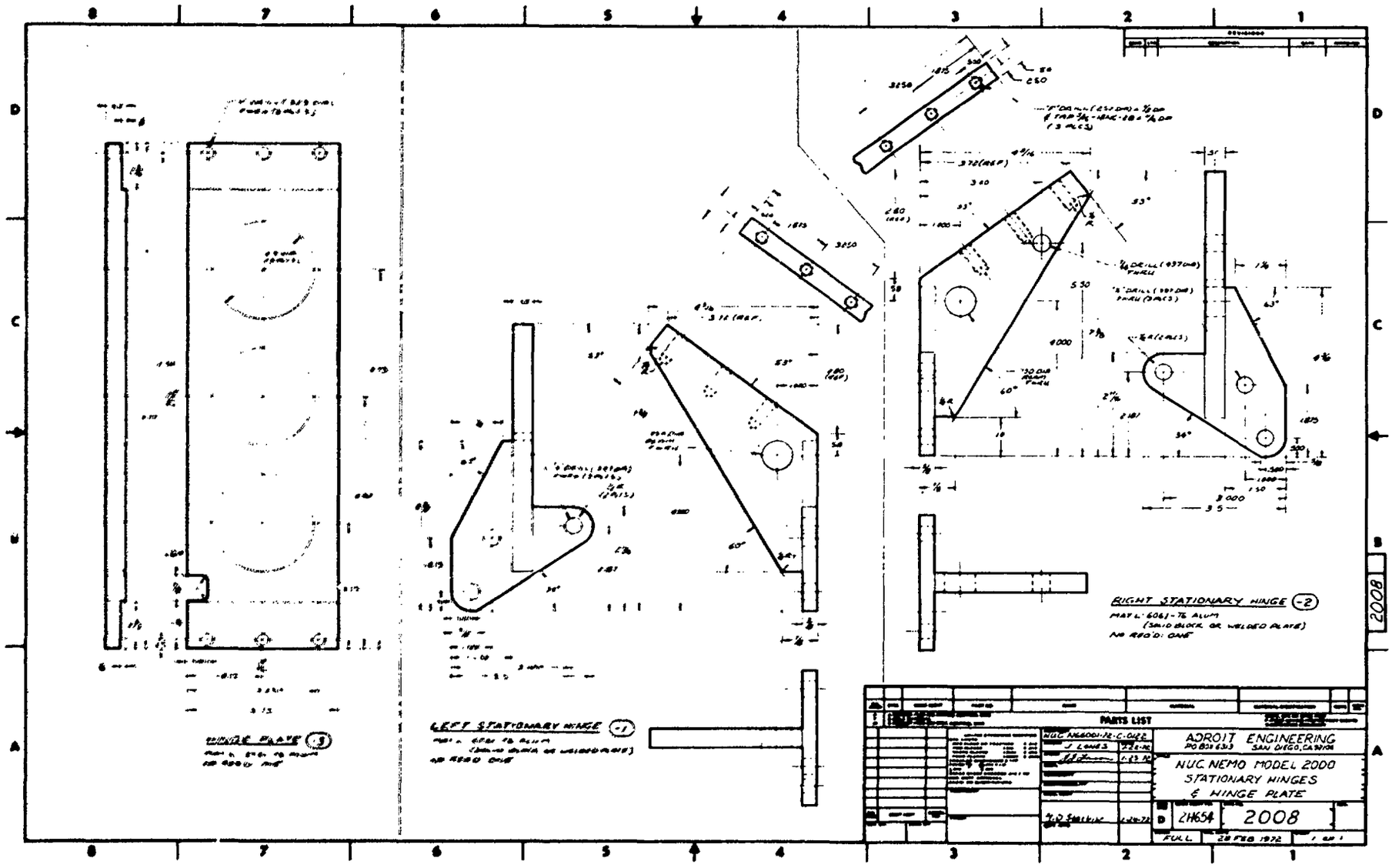
HINGE PLATE (-3)
LEFT STATIONARY HINGE (-1)
RIGHT STATIONARY HINGE (-2)
MAT'L: 6061-T6 ALUM
(SOLID BLOCK OR WELDED PLATE)
NO REQ'D: ONE
PARTS LIST
ADROIT ENGINEERING
PO BOX 6313 SAN DIEGO, CA 92106
NUC NEMO MODEL 2000
STATIONARY HINGES
& HINGE PLATE
21H654
2008
FULL
28 FEB 1972

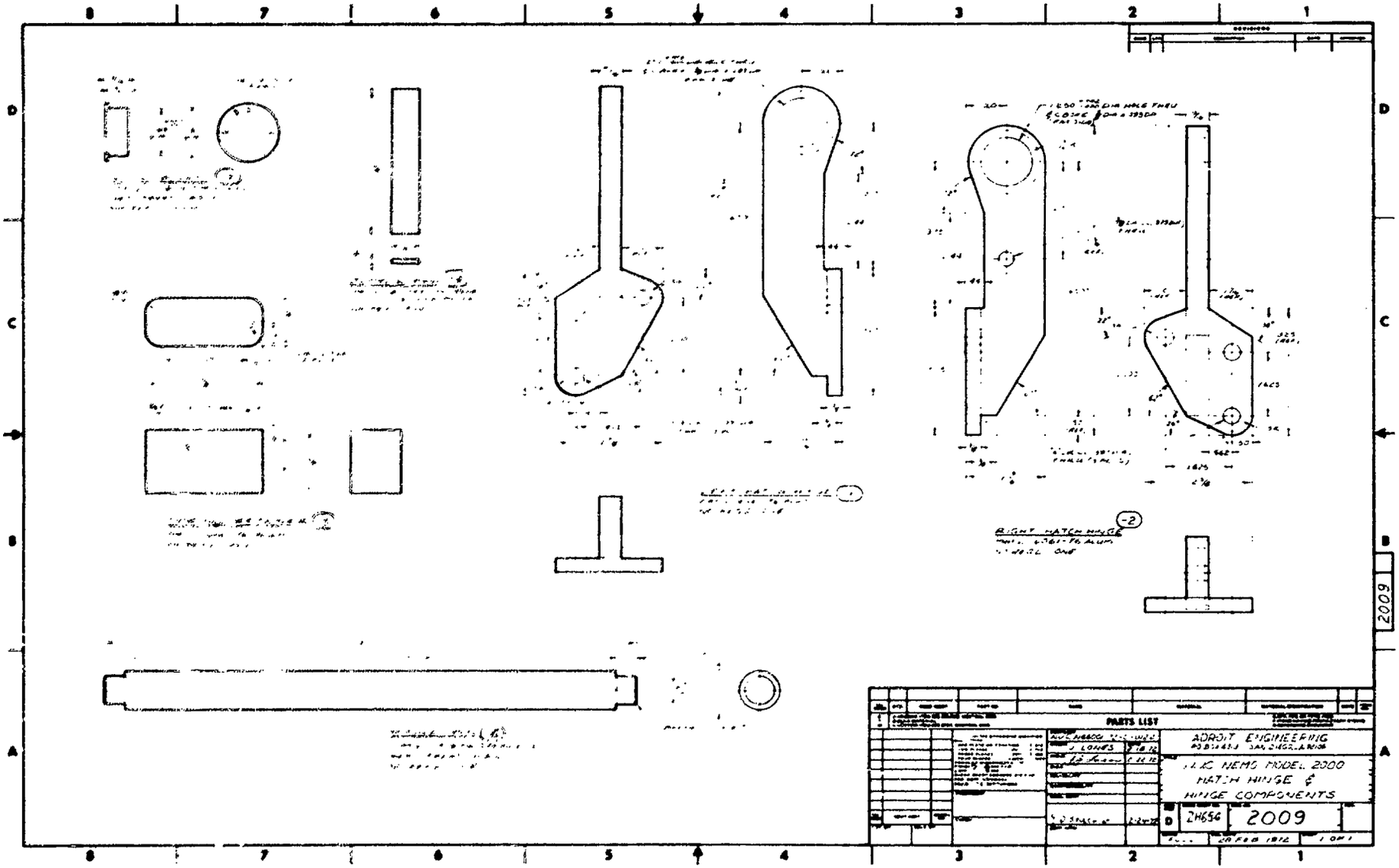
PARTS LIST
ADROIT ENGINEERING
U.K. NEMS MODEL 2000
HATCH HINGE &
HINGE COMPONENTS
2H656
2009

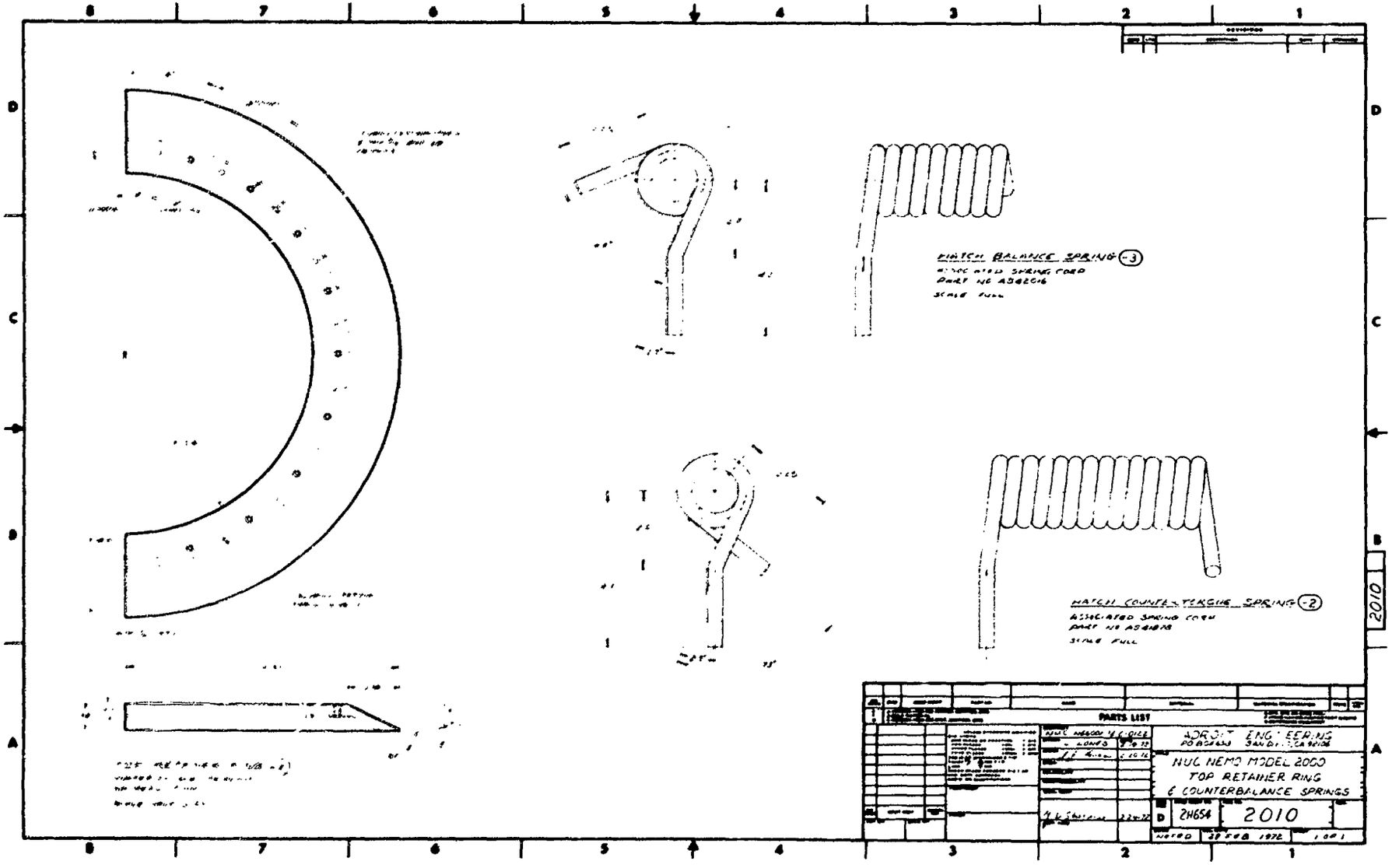
HATCH BALANCE SPRING (-3)
HATCH COUNTERTORQUE SPRING (-2)
PARTS LIST
ADROIT ENGINEERING
NUC NEMO MODEL 2000
TOP RETAINER RING
6 COUNTERBALANCE SPRINGS
2H654
2010

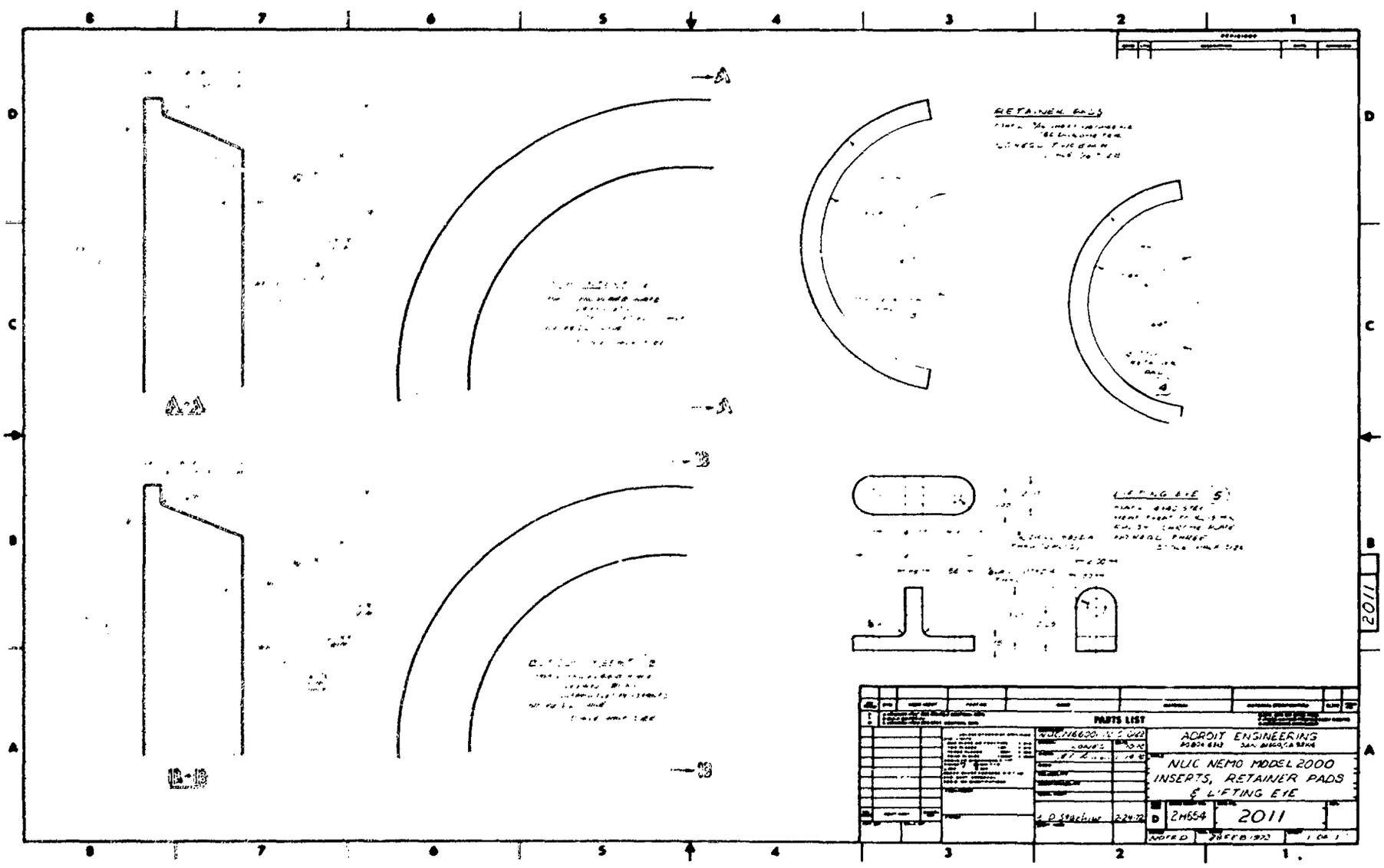
A-A
B-B
RETAINER PADS
LIFTING EYE
PARTS LIST
ADROIT ENGINEERING
NLIC NEMO MODEL 2000
INSERTS, RETAINER PADS
& LIFTING EYE
2M654
2011